Computational Analysis of Binding Preferences of PICK1 for its PDZ Partners

by

Behiye Tuğçe YILDIZOĞLU

A Thesis Submitted to the
Graduate School of Sciences and Engineering
in Partial Fulfillment of the Requirements for
the Degree of

Master of Science
in
Computational Sciences and Engineering

Koç University

October 2012

Abstract

Protein interacting with C kinase (PICK1), an evolutionarily conserved protein through animal kingdom, interacts with over 60 proteins, including receptors, transporters, kinases and ionic channels. It possesses a wide repertoire of functions, from regulation of subcellular targeting of proteins to scaffolding for assembly of multimeric protein complexes. Being a critical player in synaptic plasticity, development and neural guidance, it regulates the trafficking and posttranslational modification of its interacting proteins which take part in neuronal function. Correspondingly, the role of PICK1 in disorders such as epilepsy, pain, brain trauma and stroke, drug abuse and dependence, and schizophrenia has come into prominence with accumulating evidence from recent research.

This project concentrates on PDZ domain interactions of PICK1. Conventionally, PDZ domains fall either one of the three different subtypes, Type I, II and III, defined by the amino acid profile of the 4-residues peptides to the C-termini of their partners. PICK1 is rather unique since it interacts with both Type I and Type II partners besides atypical ones. To understand this behavior, PICK1-peptide complexes are constructed using peptides from known PDZ partners of PICK1 together with a set of artificially generated non-binding ones. Different protein-peptide assessment programs and energy functions, FlexPepDock, PepCrawler and XScore, are used to evaluate the complexes in search for consistency and correspondence with previous experimental studies. Through comparison of these different tools, peptides with higher binding affinities are aimed to be filtered. Additionally, analyzing both wild type PICK1 complexes and the ones with point mutations on critical residues of PDZ interactions, the unconventional binding behavior of PICK1 is investigated. This knowledge could be utilized by future studies on the identification of novel partners and druggability of PICK1.

Acknowledgements

I would like to thank my advisors Prof. Dr. Özlem Keskin and Prof. Dr. Attila Gürsoy for their guidance and support. I would also like to express my appreciation for Dr. Banu Özkan's generous comments on this study.

I would like to express my gratefulness to all my friends who have shared past two years with me, Deniz Çizmeci, Selin Kanyas, Merve Sancak, Esra Aslantürk, Melis Bulutoğlu, Büşra Topal, Pelin Atıcı, Emine Güven Mayorov, Engin Çukuroğlu, Serap Beldar, Halil Peynirci, Selin Karagülle and all of my past and present office mates.

I would like to thank TÜBİTAK for supporting my master studies for two years.

Finally, no word exists to express the grandness of my gratitude to my family for their endless support and love.

Özet

Protein Kinaz C-α bağlayan protein (PICK1) evrimsel olarak iyi korunmuş ve protein reseptörleri, taşıyıcı proteinler, kinazlar ve iyonik kanallar da dahil olmak üzere altmıştan fazla protein ile etkileşime giren bir proteindir. Bu proteinlerin hücre içi hedeflemesinin düzenlenmesinden multimerik protein komplekslerinin oluşumuna kadar çok sayıda farklı işleve sahiptir. Nöronal fonksiyona sahip proteinlerin trafiğini ve posttranslasyonel modifikasyonlarını düzenleyerek sinaptik gelişim, plastisite ve nöral rehberlikte rol alır. Buna bağlı olarak PICK1'nın epilepsi, ağrı, beyin travmaları, ilaç kötüye kullanımı ve bağımlılığı ile şizofreni gibi hastalıklardaki rolü son araştırmalar ile ön plana çıkmıştır.

Bu tez PICK1 proteininin PDZ yapısal bölge etkileşimleri üzerinde yoğunlaşmaktadır. Genellikle PDZ proteinleri, hedef proteinlerinin karboksil ucundaki 4 aminoasitlik peptitlerin profilleri tarafından tanımlanan üç farklı sınıftan birine düşer. PICK1 Tip I, Tip II ve atipik hedef peptitleri ile etkileşerek sıra dışı bir davranış sergiler. Bu davranışı anlamak için, bu çalışmada bilinen PICK1hedef peptidleriyle birlikte bağlanmadığı bilinen peptitler de kullanılarak PICK-peptide kompleksleri oluşturulup incelenmiştir. FlexPepDock, PepCrawler ve XScore olmak üzere üç farklı protein-peptid kompleksi değerlendirme programı ve enerji fonksiyonu, önceki deneysel çalışmalarla tutarlılık arayışı içerisinde kullanılmıştır. Bu metodlar kullanılarak yüksek bağlanma afinitesine sahip peptitler filtre edilmeye çalışılmıştır. Ayrıca, vahşi tip PICK1 kompleksleri ve PDZ etkileşimlerinde kritik olduğu bilinen aminoasitleri mutasyona uğramış kompleksler analiz edilerek PICK1'nın PDZ etkileşimleri anlaşılmaya çalışılmıştır. Elde edilen bu bilgilerden, PICK1'ın yeni hedef peptitlerinin keşfinde ve PICK1 PDZ yapısal bölgesi odaklı ilaç tasarımı çalışmalarında yararlanılabilir.

Table of Contents

LIST OF FIGURES

LIST OF TABLES

Chapter 1
INTRODUCTION

PICK1 is a critical player in the cell interacting with more than 60 partners including GluR2, the mGluR7 metabotropic glutamate receptor subtype, Eph receptor tyrosine kinases and their ephrin ligands. Correspondingly, it possesses a wide repertoire of functions from operating of receptors, ion channels and enzymes to regulation of the subcellular localisation [1]. Though it could be seen in various pathways, most of the recent research focuses on its role in the central nervous system and related diseases, more specifically in synaptic plasticity in hippocampus. It takes part in long-term depression keeping the AMPA receptors internalized in the cell [2].

PICK1 has a single PDZ (PSD-95/Discs-large/ZO-1 homology) domain responsible for many of its interactions. PDZ domains are found in thousands of proteins and are encountered in many species from bacteria to animals. They carry out fundamental functions as in protein trafficking and construction of multiprotein signaling complexes. The interfaces where PDZ interactions occur generally involve the C-termini four residues of the PDZ partners. Furthermore, the classification (Type I, Type II, and Type III) of the interactions is done based on the properties of those residues [3]. What makes PICK1 interesting to study is its promiscuous behavior that its partners are not confined to a specific Type. It is found to interact with both Type I and II, and atypical partners as well. However it does not necessarily bind any peptide belonging to either one of these classes maintaining an unusual mode of specificity.

In this work, 69 PICK1-peptide complexes are evaluated using FlexPepDock [4] and PepCrawler [5], which are two different computational methods used for structure refinement and energy scoring. Each has its own scoring function that outputs binding energy values for the protein-peptide complexes. Binding affinity of PICK1 for the different peptides in the dataset is investigated utilizing these tools. Additionally, the change in the binding behavior of PICK1 is studied upon point mutations of the critical residues involving in the protein-peptide interaction.The complexes are further analyzed with a different scoring function, X-

Score [6]. Binding trends exhibited by PICK1 under these three scoring schemes are compared within and with each other. Peptides with highest and lowest binding affinities and the energy terms most contributing to this behavior are tried to be identified. Computational results are tried to be verified by comparing them to the experimental data when available. Through this way, the energy function best represent the experiments tried to be identified and modified to better suit for PICK1 and PDZ partners.

Literature review related to the subject is provided in Chapter 2. In this section, background information involving the structure and function of PICK1 and PDZ domains are given and recent experimental and computational studies in the field are reviewed.

In Chapter 3, dataset is given and each of the assessment and scoring tools, FlexPepDock, PepCrawler and X-Score, are explained in the methods. The scoring functions, contributing energy terms, modifications to the energy functions and selection of parameters are explained in this part.

Chapter 4 represents the results obtained with each tool and includes the discussion regarding the ranking of the peptides based on energy scores, featured energy components, prominent interactions identified by each tool and their possible structural reflections. Comparison of the tools with each other is also provided here. Performances of the tools are evaluated through resemblance to the experimental data which comprises the last section of this chapter.

Lastly, a brief summary of the work can be found in Chapter 5.

Chapter 2
LITERATURE REVIEW

2.1 PICK1 (Protein Interacting with C-Kinase 1) protein

PICK1 is a peripheral membrane protein first identified as a protein interacting with protein kinase C-α(PKCα) from a yeast two-hybrid screening [7]. It is also characterized as a scaffold protein regulating the trafficking or the activity of more than 40 proteins in mammals, including neurotransmitter receptors, transporters, enzymes or channels within the central nervous system (CNS).

Being around 400 residues in length, from 415 in humans to 504 in *Drosophila,* it is present in many animal species and conserved from *Caenorhabditis elegans* to humans [1]. Mainly expressed in brain and testis, it also was found in heart, lung, liver, spleen, kidney and muscle in smaller amounts. In most of these tissues, it is dispersed in the cytosol, more densely around the nucleus, whereas in neurons it is localized in synapses [2].
Structurally, PICK1 is unique bearing both highly conserved PDZ (post synaptic density-95 (PSD-95)/Disc large/Zonula occludens-1) domain (~90 aa) and a BAR (Bin-amphiphysin-Rus) domain (~200 aa). There are three regions separating these domains: an acidic N terminal region of 18 aa, a 40 aa linker portion in between two domains and a C-terminal region composed of acidic residues. Despite being the most diversified region, the acidic nature of C termini is a conserved characteristic through all species [1].

Being essentially a lipid binding domain, BAR domain is encountered in proteins involved in membrane trafficking, mostly endocytosis. Crystallographically it is showned that BAR domain exists as a crescent-shaped dimer, composed of six helical bundles. A complete and functional BAR domain is formed when joined by another BAR domain. Two located at the ends of the dimer and two on the concave faces, there are four positively charged groups on the structure binding the negatively charged lipid molecules [8]. PICK1 also binds to lipid molecules using this domain, generally negatively charged phosphoinositides. Other regions of PICK1 can regulate this interaction either positively or negatively. BAR domain’s lipid

binding is enhanced by the PDZ domain and the linker region whereas it is inhibited by the C-terminal. Indeed, this ability is shown to be required for the synaptic targeting of PICK1, trafficking of AMPA receptors, and synaptic plasticity. Apart from lipid binding, PICK1 interacts with several other proteins, like SNAP (soluble NSF attachment protein), GRIP (glutamate receptor interacting protein) and the membrane proximal region of GluRδ2, which are also involved in functions mentioned above [9].

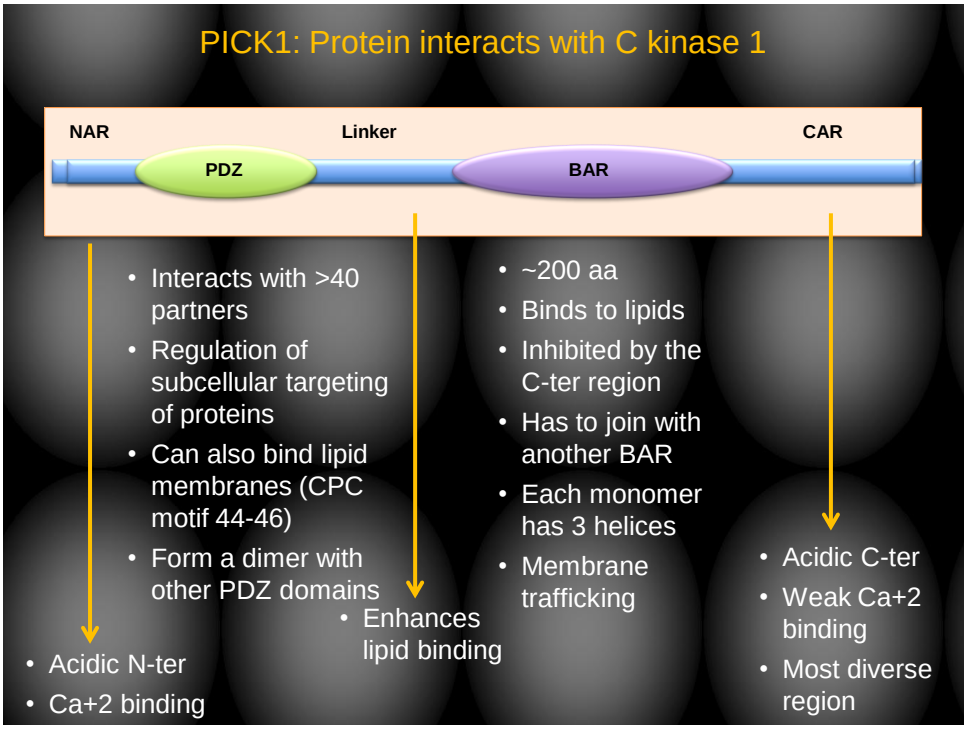

Figure 2-1 PICK1: Protein interacts with C kinase 1. Properties of domains and regions.

Apart from the modular domains, linker regions of PICK1 have also supporting functions. N-terminal acidic region was found to directly bind to Ca 2+ which affects the affinity of PICK1's interaction to GluR2 and trafficking of AMPA receptor regulated by activation of NMDA receptors [10]. Similarly, the linker region in between the two domains was found to enhance lipid binding of PICK1's BAR domain. Conversely, the acidic C-terminal region inhibits lipid binding of PICK1's BAR domain, most probably because of the interaction with the positively charged residues of the BAR domain [9]. Another

physiologically significant finding related to C-terminal region is the increased synaptic targeting of PICK1 in neurons upon its deletion [11].

Having two highly abundant modules earns PICK1 a wide repertoire of interaction partners. It is shown to associate with over 60 proteins solely through its PDZ domain most of which are involved in neural function [1]. Parallel to its high expression levels in CNS, there is accumulating evidence revealing the pivotal role of PICK1 in neural function. Its well documented interaction with AMPA receptor subunit GluR2 is required for AMPAR internalization in response to Ca2+ influx via NMDAR activation in hippocampal neurons. Additionally, PICK1 directly binds to and inhibits the activity of the Arp2/3 complex, and that this has a central role in AMPAR trafficking in hippocampal neurons.

Correspondingly, studies on PICK1's implications in various neurological disorders such as Amyotrophic lateral sclerosis (ALS) (a fatal neurodegenerative disorder characterized by the progressive and selective loss of motor neurons) [12], schizophrenia [13], chronic pain [14-17] and excitotoxic neuronal death [18] also start to stand out in literature.

However, it also possesses non-neural functions. It is shown that PICK1 functions as a negative regulator of TGF-β signaling by targeting TGF-β type I receptor (TβRI) for degradation. It interacts with the C-terminus of TβRI via its PDZ domain, scaffolding to enhance the interaction between TβRI and caveolin-1. That leads to increased caveolin-mediated endocytosis, ubiquitination and degradation of TβRI [19]. It is also shown that mutations in PICK1 gene are involved in globozoospermia, a rare congenital disease [20]. Expanding literature on PICK1 related disorders raise interest for the use of the interaction between PDZ domains and their binding partners as potential drug targets. Given that, structural information on the PDZ domains and their interactions is valuable to design suitable inhibitors.

2.2 PDZ Domain (PSD-95, Discs large, Zona occludens 1)

PDZ domain is one of the abundant modular domains existing more than 250 times in over 150 different proteins in human proteome [21]. PDZ domains are less likely to be encountered in unicellular organisms implying possible co-evolution with multi-cellularity.

There are over 300 PDZ structures currently deposited in the PDB data bank. [22] PDZ domains exhibit plethora of cellular functions from establishment and maintenance of cell polarity to regulation of cell junctions, from transmission in neurons to visual and auditive processes, from synaptic plasticity to cell migration [23-27]. This diversity of binding specificities and functional roles of PDZ domains can be attributed the considerable sequence variation they exhibit [23].

PDZ domains are 80–100 amino acids long forming six anti-parallel β strands (βA-βF) and two α-helices (αA and αB). The βB strand and αB helix form the binding pocket to PDZ-binding motifs. Peptides recognized by PDZ domains are 4-5 residues long, yet it is claimed that up to seven C-terminal ligand residues can interact specifically with the PDZ binding cleft [28]. βB strand runs the length of the peptide-binding groove and places the peptide as an additional strand into the antiparallel β-sheet on the surface of the domain with the main chain interactions it provides. Still, there is more to consider than these interactions for sequence-specific recognition by PDZs [23].

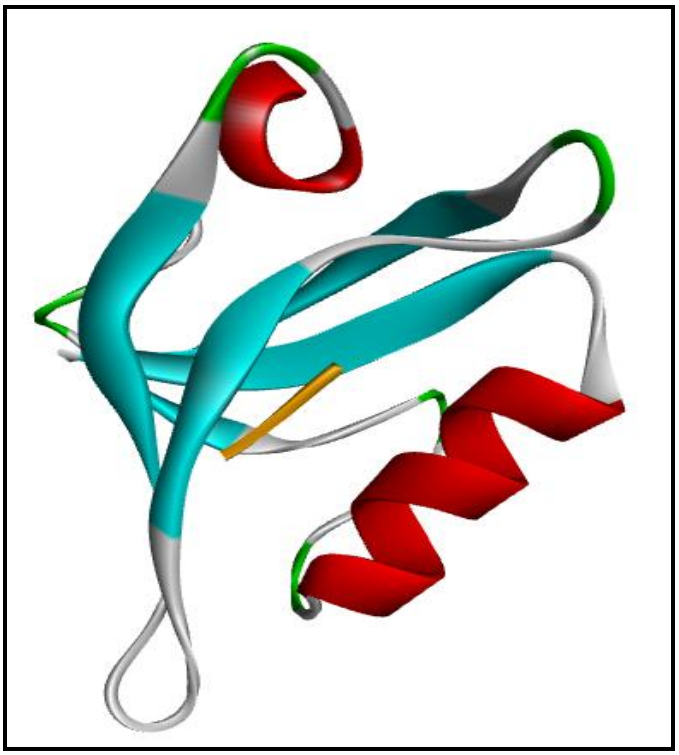

Figure 2-2 PICK1 PDZ domain in complex with the peptide (WLKV) from PDZ partner Dopamin Transporter (Figure created with Discovery Studio using PDZ domain of PDB ID: 2PKU)

PDZ-binding peptides can be divided into three classes based on their selectivity on PDZ-binding motifs, short peptides from the extreme C-termini of their substrate proteins. Type I PDZ domains recognize X-[T/S]-X-F motif, Type II domains bind X-F-X-F and Type III ones interact with X-E/D-X-F. (F-hydrophobic residue; X-any residue; T-threonine; S-serine; E-glutamate; D-aspartate.) These types were set by the residue located at the -2 position of the ligand, where the amino acids are numbered according to their topographical location, the extreme C-terminus being at position 0 (P0) [23]. Similarly, the selectivity of a PDZ domain for its ligands is determined by the first residue of the a-helix B (aB1) of the PDZ domain. Conventionally, a Type I PDZ domain has a histidine in the aB1 position, Type II holds a hydrophobic residue and Type III bears a tyrosine.

Apart from conventional C-terminal peptides an internal sequence can also bind PDZ domain forming a hairpin-like structure. PDZ domains can also form dimers with the other PDZ domains [23] and are also capable of binding to lipid molecules, such as phosphoinositides [9].

As opposed to many PDZ domain-containing proteins, PICK1 possesses a single PDZ domain. However, what makes PICK1 interesting is it being one of the few PDZ domain proteins that can bind peptides belonging different classes. Even though, initially identified as a Type I PDZ, PICK1 is found to interact with Type II and atypical peptides. [29] Sorting out this behavior of PICK1 has implications in domain-peptide interactions, peptide binding specificity and drug targeting.

2.3 Previous experimental studies

Experimental efforts for investigating the binding preferences of PDZ domains and the features of the peptides interacting with PDZs of different proteins include high-throughput technologies like phage display [21, 30] and protein microarray [31]. A phage display study on human and worm PDZ domains classified them into 16 conserved specificity groups [21]. Alternatively, in one protein microarray study most of the mouse PDZ domains were purified to determine their binding specificity against 217 peptides collected from the C-terminal of mouse proteins. As a result it was suggested that the

selectivity space of PDZ-peptide interactions are rather continuous, as opposed to the discrete classes approach. Also, discrimination between binding and nonbinding peptides was used in an effort to predict the PDZ-peptide interactions [31]. The mouse binding data is further utilized in training of a model for prediction of PDZ-peptide interactions in *D. melanogaster* and *C. elegans* [32].

However improved the techniques, experimental binding specificities are still difficult to obtain and computational approaches to the peptide binding specificity problem are essential. Using computational biology tools in effort to elucidate the binding behaviors of PDZ domains and in the prediction of undiscovered interaction partners with the use of experimental data is currently a growing area of research.

Unconventionally capability of binding Type I, Type II and atypical peptides, what accounts for this behavior of PICK1 was investigated by several studies before. In a highly referred study by Madsen et al., characteristics of the PICK1 PDZ binding pocket is investigated using fluorescence polarization based binding assay. Interactions carried out by each residue of representative Type I and Type II peptides are analyzed. Contributing residues and interactions and the effects of mutations of critical residues, Lys27 and Lys83, on these interactions are analyzed [33]. In another study employing the same technique, a small molecule inhibitor binding in an irreversible but specific manner to PICK1 PDZ domain is detected indirectly providing information on binding preferences [34]. A study exploring explicitly the potential binding partners of PDZ domains of PICK1, GRIP and syntenin discovered new glutamate receptor subtype partner for PICK1 and utilize that data to shed light on structural determinants of PDZ interactions [27].

Regarding the elucidation of the important residues on the PICK1 domain, in an *in vitro* study Ser 77 is found to be a major phosphorylation site for PKCα which is an notable mechanism regulating the activity of PICK1 [35]. Additionally, Thr82 is shown to be a potential phosphorylation site and important for the interaction between PICK1 and AMPA receptor, GluR2 [36].

Though there is increasing experimental evidence revealing new interaction partners of PICK1, this data is not analyzed for complete understanding of the binding behavior of PICK1. Investigation of the known binding partners of PICK1 collectively and in comparison

with each other can help elucidating the critical interactions and preference towards different Types. Incorporation of experimental findings into computational analysis can enhance the performances of the computational tools in representation of the current data and in the prediction of novel binding partners.

2.4 Previous computational studies

Being one of the heavily studied domains, there is considerable amount of PDZ specificity data available. This knowledge is appraised computationally by various algorithms for the prediction of binding specificities of peptide-binding domains and for the prediction of their natural ligands. Computational tools like docking, generating conformational ensembles [37] are also used to elucidate the promoting interactions and residues, and to more elaborately explain the binding preferences of PDZ domains for different peptides. Various computational methods such as statistical and machine learning approaches, biophysical and computational chemistry methods were utilized for these purposes, as reviewed recently [38].

One example for the methods used for prediction is Position Weight Matrices (PWMs) in which each cell holds the probability of observing an amino acid at a given ligand position to acquire a score describing the binding preference of a PDZ domain for a given peptide. In one such study, PWMs are used to predict the peptide binding specificity of different human PDZ domains [21]. Another work involves a machine learning method called a support vector machine (SVM) to achieve the same goal and tested with human, worm and fly proteomes, claiming % 85 accuracy with human PDZ domains [39]. In another effort, bayesian estimation is shown to accomplish ~%80 true positive rate in prediction of novel Mouse PDZ domains and peptides given the PDZ domain and peptides' primary sequences. [32] In one study specifically concentrated on PSD-95 PDZ domain, a more complex protocol involving quantum mechanics/molecular mechanics, semi-empirical Poisson–Boltzmann/surface area and empirical conformational free energy analysis is proven to recreate the experimental data of 30 affinity-known PDZ3–peptide complexes, besides providing information on energetic profile and structural basis of peptide binding [32].

Though there are computational methods on classification and prediction for PDZ domain peptides in general, PICK1 has not been handled before specifically except a few studies. In one such case, 44,000 compounds were first screened with fluorescent polarization assay to find a small molecule inhibitor where FSC231 is shown to achieve this. Its binding mode was found using computational docking. In a subsequent work, structure activity relationship for this compound was studied again utilizing docking methods and a derivative structure with higher affinity was reached [40, 41].

In another study involving peptide partners of PICK1 PDZ domain, binding affinities of all major PICK1 partners and the effects of PICK1 mutations on those are investigated by Perturbation Response Scanning and ensemble docking with RosettaLigand. Featured residues and interactions contributing to the peptide binding specificity are searched out providing for potential drug design studies [42].

Another computational work puts the problem into binding free energy landscape frame using Monte Carlo simulations to describe peptide binding process of PICK1 PDZ domain and two other PDZ domain proteins, PSD95 and GRIP. It was suggested that binding occurs in a two-step mechanism with the P(0) binding to the peptide binding pocket as the initial rate limiting step. Also, PICK1 PDZ binding to the Type I peptide is shown to involve a lower free energy barrier than the Type II peptide [43].

Though, there is different lines of computational work on the subject, there is none representing the performance of available tools specifically for PICK1. The capabilities of the current computational tools on this aspect and potential features for improvement can be explored for the more efficient use of these tools on the specific case of PICK1. This is aimed to be achieved in this study with the use of a larger dataset and incorporation of mutational analysis differently from previous studies.

Chapter 3
MATERIALS AND METHODS

3.1 Dataset

The experimental structure of the complete PICK1 is not available yet. However, there are four PICK1 PDZ Domain structures deposited in PDB. Among those, two are used in this study, 2GZV [44] and 2PKU [45]. 2GZV is a crystal structure used previously in similar studies. [42] Yet, it has an unresolved portion and a more recent and complete structure, 2PKU, is available in PDB. 2PKU is the NMR structure of PICK1 PDZ domain deposited in PDB as an ensemble of 20 models. It covers the residues between 18 and 104 of PICK1 in complex with five GluR2 C-termini residues [-ESVKI]. The average structure is determined using Discovery Studio 3.1 and the further analysis is done with this structure.

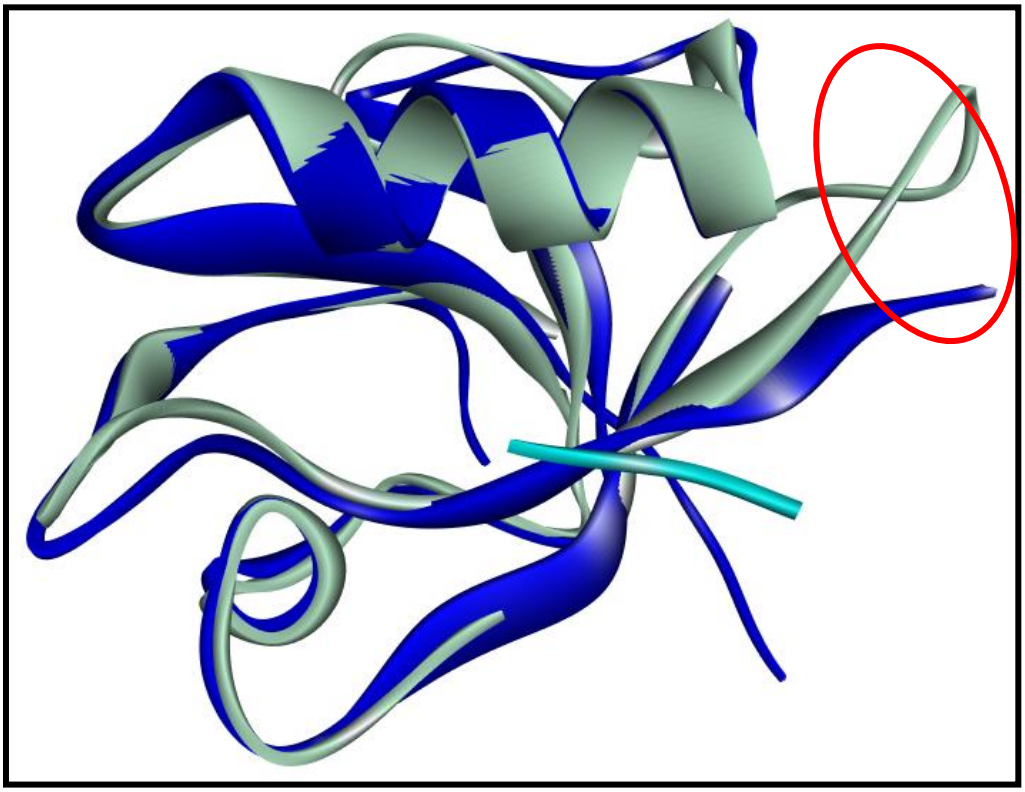

Figure 3-1 2PKU (grey) and 2GZV (blue) superimposed. The GluR2 peptide ESVKI of 2PKU is shown in turqouise. Missing portion is marked with red circle.

3.1.1 PDZ Peptides

Type I, Type II and also atypical PDZ binding and non-binding peptides are collected from previous studies available in literature [27, 29, 33, 42]. Additionally, computationally generated Type III and atypical peptides are included in the dataset. Since PICK1 does not have any Type III partners, artificial Type III peptides are generated by mutating the Type I peptides in hand and used as negative data for further comparison. Complete list of peptides is presented in Table 3-1.

Table 3-1 Peptides used in the study. Peptides collected from literature are coming from experimentally verified complexes. Artificially constructed peptides are generated by introducing mutations on the Type I peptides

Collected from literature					**Artifically constructed**	
Type I	**Type II**		**Atypical**	**Non-binding**	**Type III**	**Atypical**
DSLV	EWYV	AMPV	DFTC	DSSL	EECI	ETCG
ETCI	GIQV	DVPV	EAEC	WLKD	EEMA	ETMR
ETMA	IPEV	EIAC	KKNK		EEVA	ETVC
ETVA	PMPV	LNAV	MKPK		GDIV	GSIK
GSIV	SFVL	NLVI	PPTV		GDKA	GSKH
GSKA	SIKI	SVEV	RNQK		NEVV	NTVK
NTVV	VDV	SVIM			QDAV	QSAK
QLAV	WFDV	SVKI			SEYV	STYC
QSAA	WLAI	SVSV			TDSL	TSSD
QSAI	WLKI	SVVI			TERV	TTRE
QSAL	WLKL	TVSV				
QSAV	WLKV	WLKA				
STYV	YYKV					
TSSL						
TTRV						
WSKV						

PICK1-peptide complexes are first constructed in Discovery Studio 3.1. This step does not involve any docking or energy calculation, rather the complexes were built by mutating the peptide in the original 2PKU PDB structure in place. To remove the clashes in

these initial complexes, they are pre-processed with either Prepack or ClassicRelax routines in Rosetta software version 3.2.1[46].

In addition to wild type complexes, PICK1 PDZ domains with point mutations on critical residues are studied. There are previous studies, both experimental and computational, investigating the effect of K27A, K27E, K83H, K83V and T82E mutants on binding affinity of PICK1 PDZ domain for various peptides [33, 36, 47, 48]. Accordingly, those complexes are recreated to see if the results could be reproduced with the tools used in this study for the assessment of protein-peptide complexes.

3.2 Assessment of the PICK1 PDZ-Peptide Complexes and Energy Calculations

To investigate the binding behavior of PICK1, PDZ-peptide complexes are evaluated with three different docking routines/structure assessment tools, namely FlexPepDock [4, 46], PepCrawler [5] and XScore [6].

3.2.1 FlexPepDock

FlexPepDock protocol is an algorithm in Rosetta library for generation of high-resolution models of complexes of flexible peptides and globular proteins, given an approximate, coarse-grain model. It was benchmarked over a large dataset of peptide-protein interactions and showed high success rates in sampling sub-angstrom (%87 in a range of 3.5 Å bb Root-mean square deviation (rmsd)) and near-native models (%91 in a range of 5.5 Å bb rmsd). Moreover, the protocol has achieved to sample the sub-angstrom models when tested for cross-docking with a dataset of PDZ-peptide complexes, suggesting it would be a suitable tool to study PICK1-PDZ peptide complexes [49].

As the first step of FlexPepDock protocol, the preliminary complexes are fed to the prepacking routine for the removal of the internal clashes. Subsequently, the second step, peptide docking mode, involves the optimization of the peptide backbone and its rigid-body orientation relative to the receptor protein, in addition to simultaneous side-chain optimization. The number of decoys (i.e. conformations of the complex) to be generated by setting how many times this step is to be repeated can be set here. This step also includes an

optional low-resolution (centroid) pre-optimization mode. In the end, the output models are ranked based on their energy score according to the Rosetta score12 energy function.

To search for the capabilities of the tool and to improve the results based on the experimental data, the effect of several FlexPepDock parameters are tested. Computational experiments are carried out with generating different number of decoys, introducing different constraints to the complexes and changing the weights of the energy terms in the evaluation of the complexes.

3.2.2 PepCrawler

PepCrawler is an algorithm which derives peptides from protein-protein complexes and predicts protein-peptide complexes by high resolution docking and binding affinity estimation. It primarily aims to aid detection of inhibitory peptides for protein-protein interactions. It allows backbone flexibility for the peptide combined with side-chain flexibility for both the peptide and the receptor protein.

Provided the receptor and the ligand, the algorithm derives a single, short, low-energy binding peptide in the first step. Second, it generates a large amount of peptide docking conformations and explores the conformational space by using RRT-based algorithm and grid-based collision detection. Then, it scores and clusters these conformations, and outputs the top five cluster candidates. In the third step, a more refined RRT with less peptide flexibility is carried out around the conformation of each cluster candidate. The backbone-atom RMSD (bb-RMSD) between the highest scoring conformation of the input peptide and each of the other conformations is calculated.

3.2.3 X-Score

To see if the binding affinities of PICK1-peptide complexes exhibit differences under different energy schemes, resultant structures from FlexPepDock protocol are evaluated with another assessment tool, X-Score, for further comparison.

X-Score is a consensus empirical scoring function for estimating the binding affinity of a given protein-ligand complex with a known three-dimensional structure. It incorporates van der Waals interaction, hydrogen bonding, deformation penalty, and hydrophobic terms in

to the function. Providing binding energies (kcal/mol) and predicted binding affinities (log K_D) for complexes X-Score combines three different scoring functions. It is shown to predict the binding free energies with a standard deviation of around 2kcal/mol and to perform better in identifying the correct bound conformation than the classical force field calculation [6].

Chapter 4
RESULTS

4.1 FlexPepDock

The first concern in running the FlexPepDock is to determine the number of decoys to be generated to overcome the tradeoff between the computational power in hand and enough sampling. Conventionally, at least 200 to a optimal 2000 decoys are created in FlexPepDock runs. However, it was not possible to achieve this number due to computational limitations. Then, experiments with various number of decoys are carried out to determine the smallest plausible value. For a few complexes 100, 500, 1000 and 5000 decoys are generated as test cases. Assuming 5000 already samples good enough, 500 is determined to be the smallest required value to cover the same space and to provide the similar convergence that 5000 decoy runs achieve. One Type I (QSAV) and one Type II (WLKV) peptide-PICK1 complexes are chosen as representative to demonstrate the results. (Figures 4-1, 4-2)

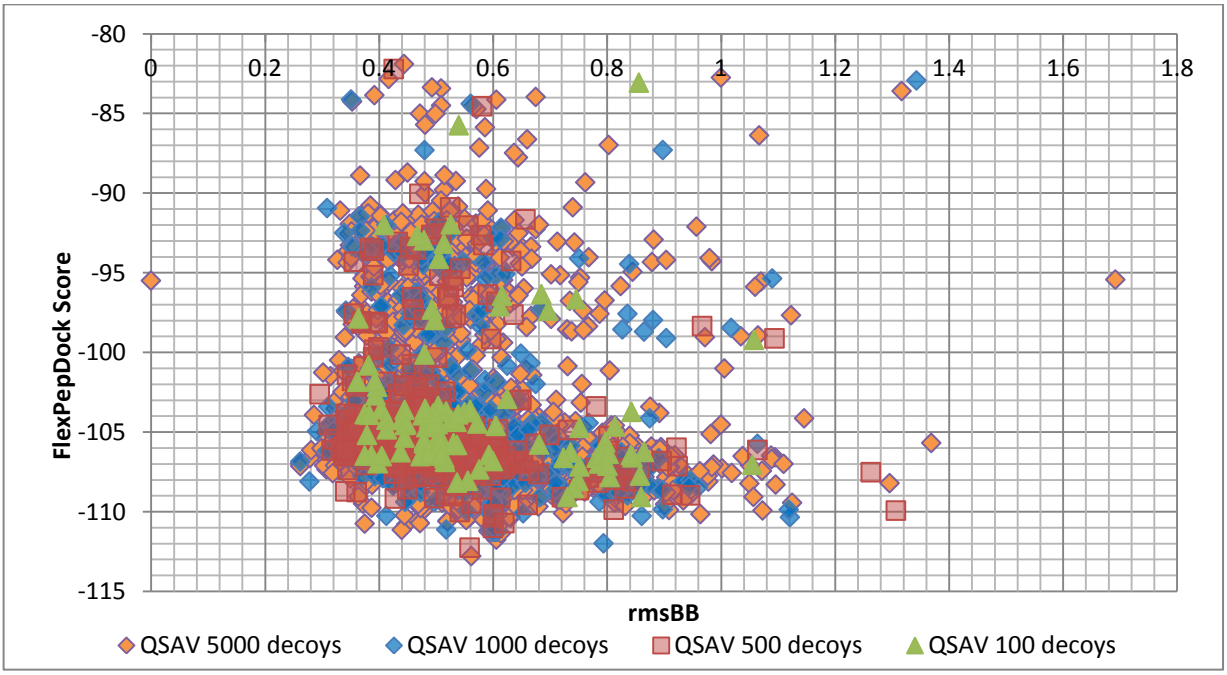

Figure 4-1 Distributions of FlexPepDock scores of decoys versus Backbone RMSDs to initial structure of Type I peptide (QSAV) complex for 100, 500, 1000 and 5000 decoy cases

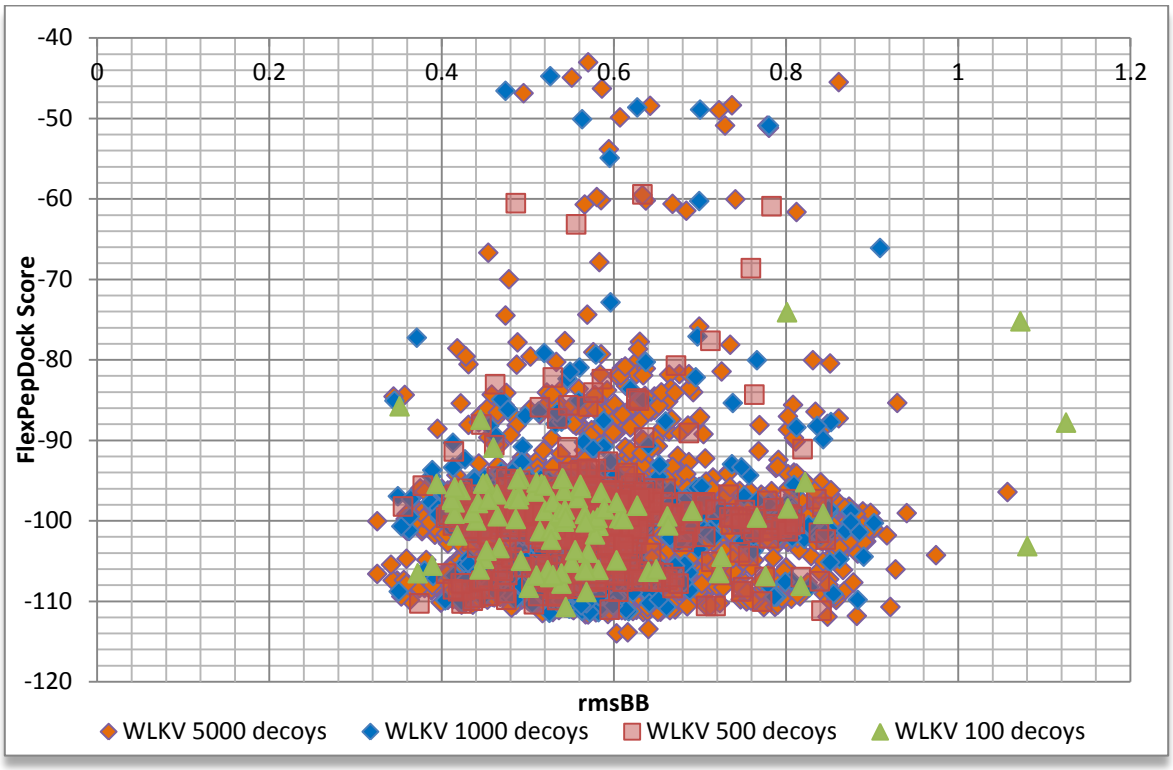

Figure 4-2 Distributions of FlexPepDock scores of decoys versus Backbone RMSDs to initial structure of Type II peptide (WLKV) complex for 100, 500, 1000 and 5000 decoy cases

Once the number of decoys to be generated is set to 500, then the complete dataset (Table 3-1) is evaluated to see if the binders could be separated from non-binders. Since there is no experimentally determined affinity data for all of the complexes, it is not possible evaluate each of them individually, rather the complexes are evaluated comparatively. DSLL, shown to be a non-binder experimentally in a previous study, is chosen as marker. Then the binders and non-binders are evaluated compared to DSLL. Though, scoring close to DSLL most of the known binding peptides have lower binding energies than it has (Fig 4-3). Strikingly, all of the Type III peptides have more unfavorable energies than DSLL, supporting the notion that PICK1 having no Type III partners. Type II peptides seem to be favored binding partners compared to the others, most members having lower binding energies relative to the other types. However, what is more striking is the distribution of the rmsd values of the complexes.

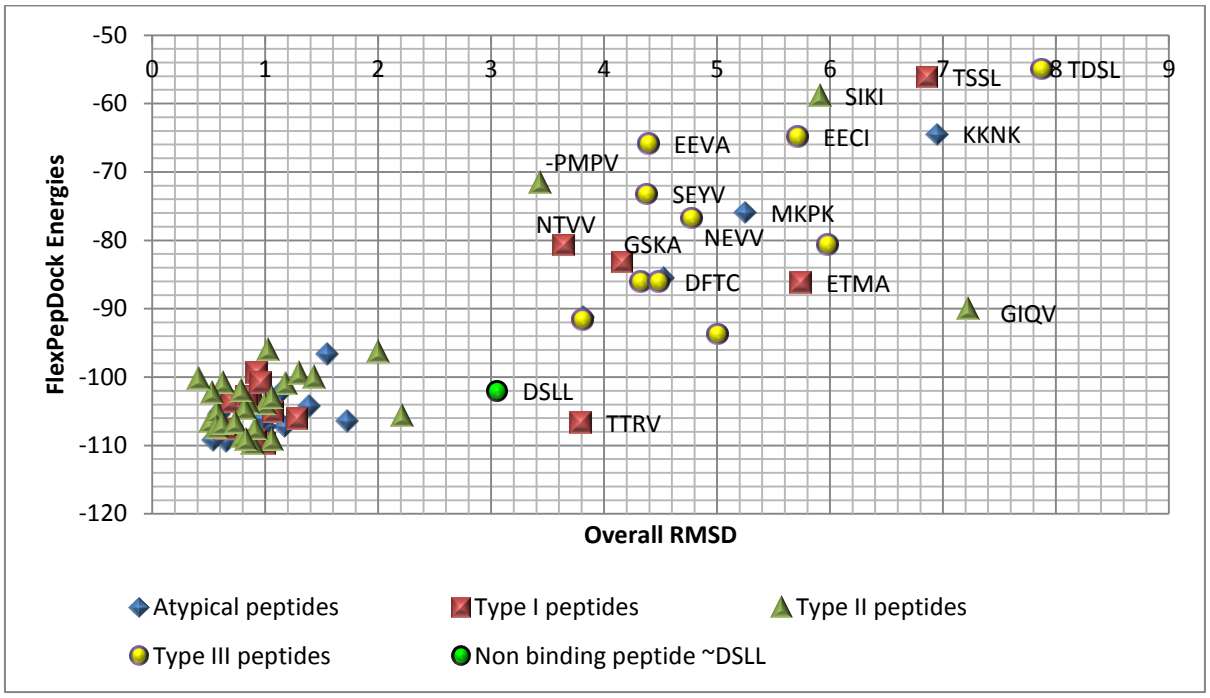

Figure 4-3 Distribution of Type I, Type II, Type III and Atypical complexes based on the FlexPepDock scores when no constraints are introduced. On the x-axis RMDSs over all atoms of the minimum energy decoy to the corresponding initial structure are plotted. Each point on the plot corresponds to the complex of PICK1 with a peptide as listed in Table 3-1. (Complete data available in Appendix Table 5-1)

Though most of the higher rmsd complexes also have higher energies, an rmsd based comparison makes a more obvious separation. All Type III complexes then have rmsd values larger than the DSSL complex yet some known binding partners appear among non-binders. Relatively larger deviations in these structures implied by larger rmsd values can be caused by initial structure being a Type II peptide complex. Therefore, to locate Type III peptides in the binding pocket, the structure is forced to change more, whereas Type I and Type II peptides are more easily positioned. Indeed, in high scoring structures repulsive terms constitute the greatest contribution to the increase in the energy score, though the involving residues vary among the complexes. For instance in ~EECI complex, Cys in P(-1) is mostly responsible for the high repulsive term together with more moderate contribution of Ala87 and Ile35. This implies that Cys could not be located optimally to the binding pocket which also explains the high rmsd value. (Figure 4-4) On the other hand, the major contributive of the high score of EEVA complex is the Glutamic acid in P(-3) and P(-2) to a smaller extend.

Even differently, Val in P(0) turned out to be reason for the high score of NEVV complex disturbing Leu32 and Lys in the same position in KKNK complex creates a similar case with Ala87. A further investigation of the worst scoring complex, TDSL, reveals Thr as the source of unlikely high energy of the complex. The PICK1 residues surrounding P(-3) Thr, which are Lys83, Val86, Ile70, Leu47, Tyr48 and Ile37, appears as unable to position the residue, since they also contribute highly to the repulsive term of the complex. Similarly, in case of TSSL the major cause of the unfavorable energy is Thr besides the smaller contribution of Ser in P(-2). The residues around Thr in P(-3), same as those in TDSL complex, also have relatively high repulsive terms implying it's difficulty in fitting the binding pocket. In order to avoid these several constraints and scoring schemes are tested discussed further below.

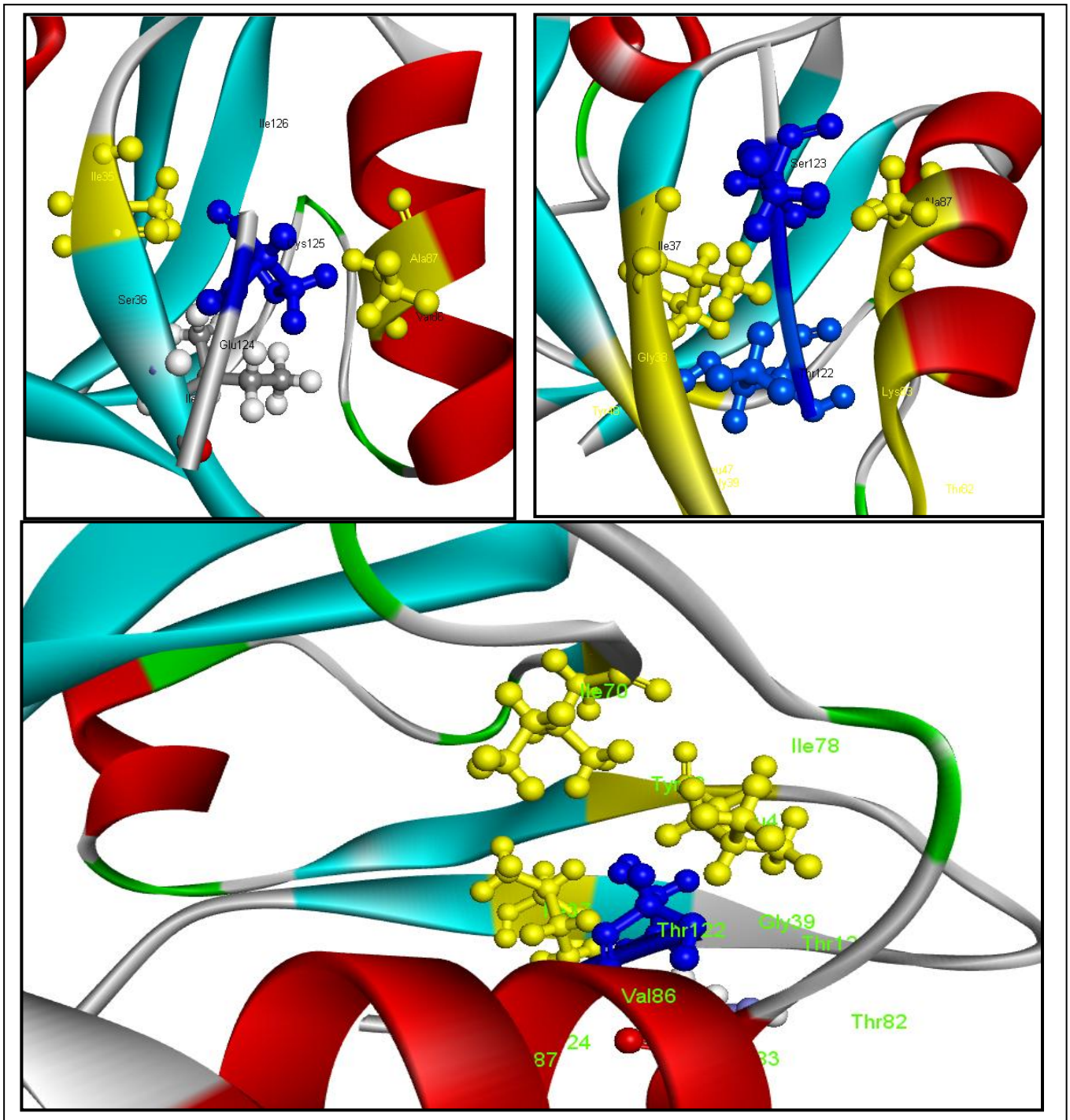

Figure 4-4 Close up to the binding pockets of the complexes with the highest binding energies according to FlexPepDock. The peptide residues contributing most to the high scores are represented in blue and the surrounding PICK1 residues with high repulsive components are shown in yellow. Upper left figure belongs to KKNK complex, the highest scoring atypical complex. TSSL complex is represented to the right and TDSL complex, the one with the most unfavorable energy, is shown larger at the bottom.

Several type-specific interactions are introduced as constraints to the complexes in effort to sort out different Types of peptides. 4 different sets of constraints were compared, (1), securing the H-bond between the P(-2) residue of the peptide (either Ser or Thr) and Lys83 of the PDZ domain, which is specific to Type I (Constraint I), (2) preserving the hydrophobic interaction between P(-2) of the peptide and Lys83 (specific to Type II) (Constraint II), and (3) fixing the interaction between Gly34 and P(0) residue of the peptide which is common to all types (Constraint III). Combination of P(0) to Gly34 and Ile35, and P(-2) to Lys83 and Ala87 interactions is given as the last set of constraints (Constraint IV). In all cases, constraints are set as harmonic with a standard deviation of 2.0 Å.

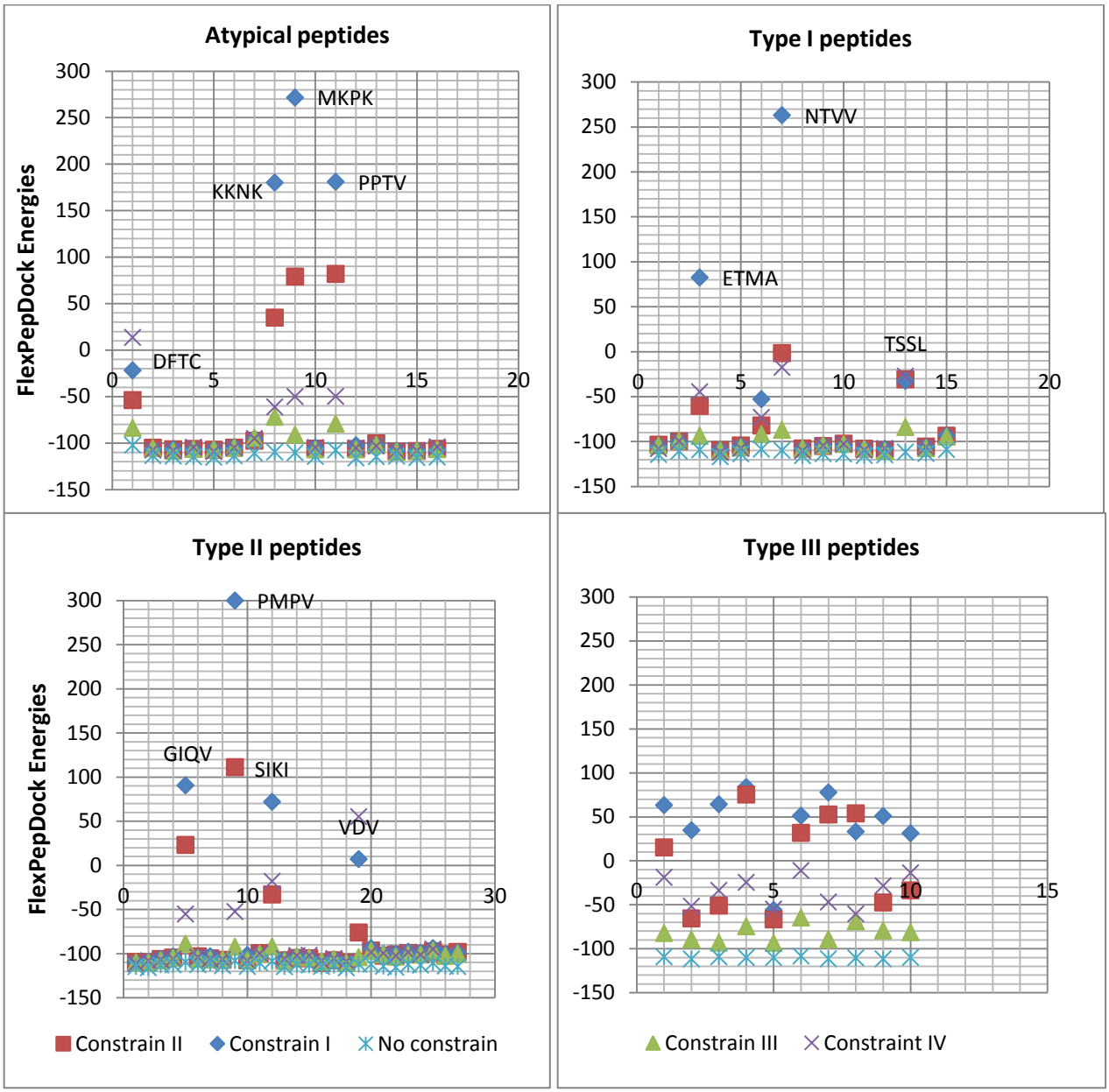

Figure 4-5 Energies of the Atypical, Type I, Type II and Type III complexes upon implementation of three different sets of constraints in the FlexPepDock routine. Peptides are indexed on the x-axis as listed in Table 3-1. (Data available in Appendix Table 5-2)

Different sets of constraints are observed to cause similar effects on the energy profiles of the groups of Type I, II and Atypical peptides. (Figure 4-5) The energies of these complexes are not altered significantly upon implementation of Constraints I, II, III, IV, except for a few cases where the same complexes have relatively high energies independent of the constraint type (Sequences are labeled explicitly on Figure 4-5). A closer attention on

these complexes reveals that they are also the ones with the most unfavorable energies when there are no constraints. (refer to Figure 4-4). This might imply that constraints further limit the flexibility of these structures which are already forced in the absence of constraints. Thus, introducing constraints raises the energies of the complexes even higher.

Implementation of Constraint I and Constraint II causes larger binding energies than Constraints III and IV does. Constraints I and II restrict the P(-2) residue which is responsible for the large repulsive term in most of the high scoring complexes in no-constraint cases. Therefore, this might further decrease the flexibility of the peptide in those complexes and making it harder to encounter lower energy decoys. Operating on the already better positioned P(0) Constraints III and IV causes smaller changes in binding energies. This may imply that P(0) can be more readily fit to the binding pocket even in the absence of constraint. Following that it could also be said that adding constraints in the case for higher energy structures is actually forcing the structure and cause even higher energies.

The energies of the Type III peptides however decrease when Constraint III is applied. Presumably increased binding tendency of otherwise non-binding Type IIIs can then be attributed to the critical interactions of the P(0) binding pocket which is conserved for all peptides regardless of the type. The increase in energies where type specific interactions are tried to be maintained through Constraint I and II, also supports this. Also, the binding energies of the Type III complexes under Constraint IV range between those of Constraint III and of Constraint I/ II. This could point out the contribution of the P(0) interactions in determination of binding and non-binding PDZ peptides without discrimination of the type of peptide.

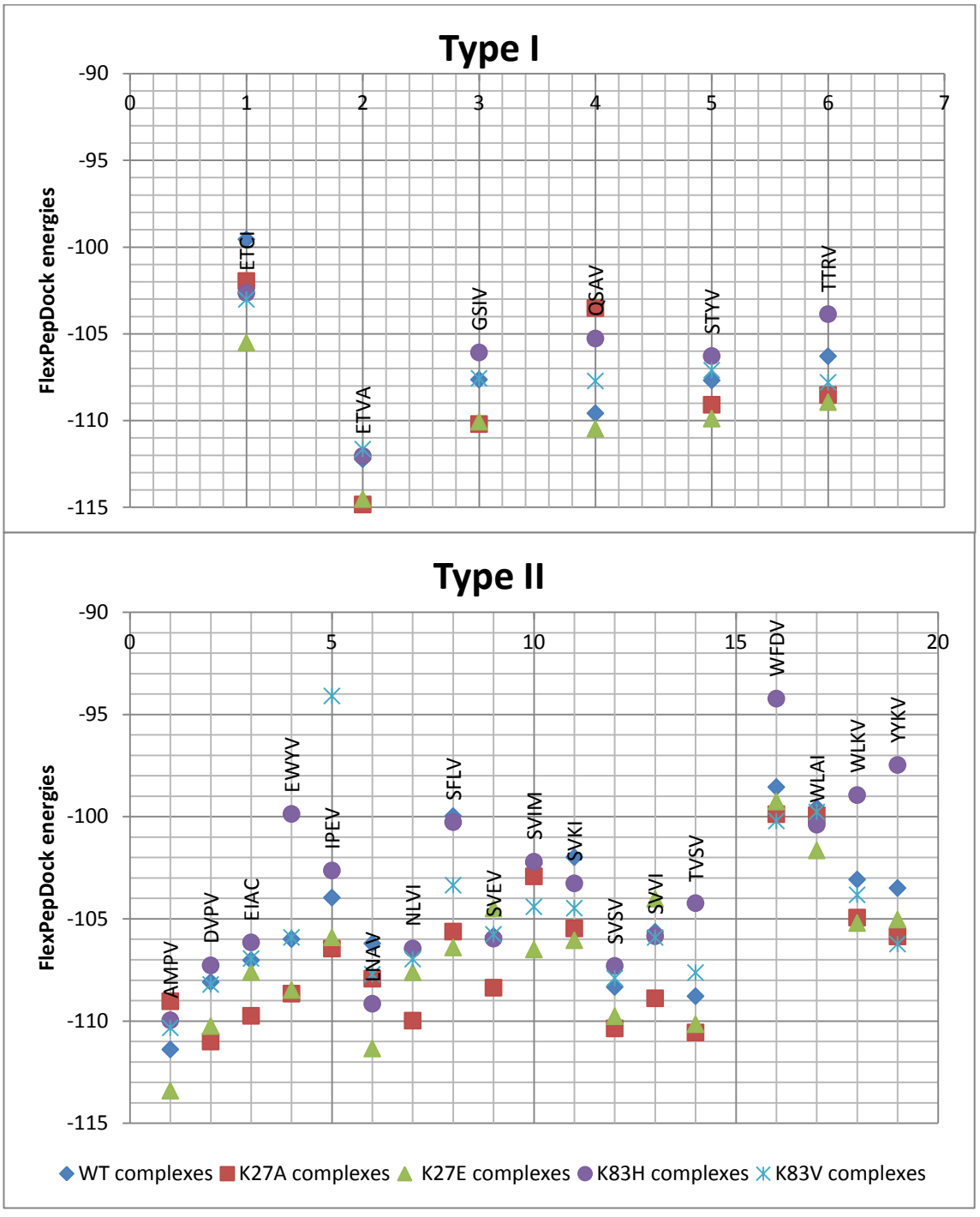

Figure 4-6 FlexPepDock energies of PICK1 PDZ domain WT and K27A, K27E, K83H and K83V mutant-Type I and Type II peptide complexes (Complete data available in Appendix Table 5-3)

To investigate the binding preferences of PICK1 PDZ for it partners of Types I and II PDZ peptides, mutations are introduced on the critical residues, Lys27 and Lys83, involving

in the protein-peptide interactions. Lys27 carries out interactions in P(0) binding pocket involving in the carboxylate binding loop. It also contributes to the commonly found KD motif in Type II PDZ domains. Bearing a Lysine83, in the critical αβ1 position, PICK1 does not fit the conventional Type I and II classes, for Type I generally require a His in this position whereas in Type II a hydrophobic amino acid occupies it. P(-2) residue is responsible for this preference since Ser/Thr of Type I H-bonds to αβ1 and a hydrophobic P(-2) carries out hydrophobic interactions with it.

WT and K27A, K27E, K83H and K83V mutant complexes are processed with FlexPepDock to see the change of preference of PICK1 for Type I and II partners upon these variations (Figure 4-6). According to the preference based on αβ1 residue, K83H is supposed to promote the binding of Type I peptides whereas K83V should favor Type II peptides. This trend is caught with the Type II peptides where K83V mutation lowers the binding energy relative to the WT in most of the complexes and K83H complexes are the most unfavorable ones for all complexes. However, Type I peptides do not follow the expected trend since only one of the complexes (ETCI) showed improvement upon K83H mutation.

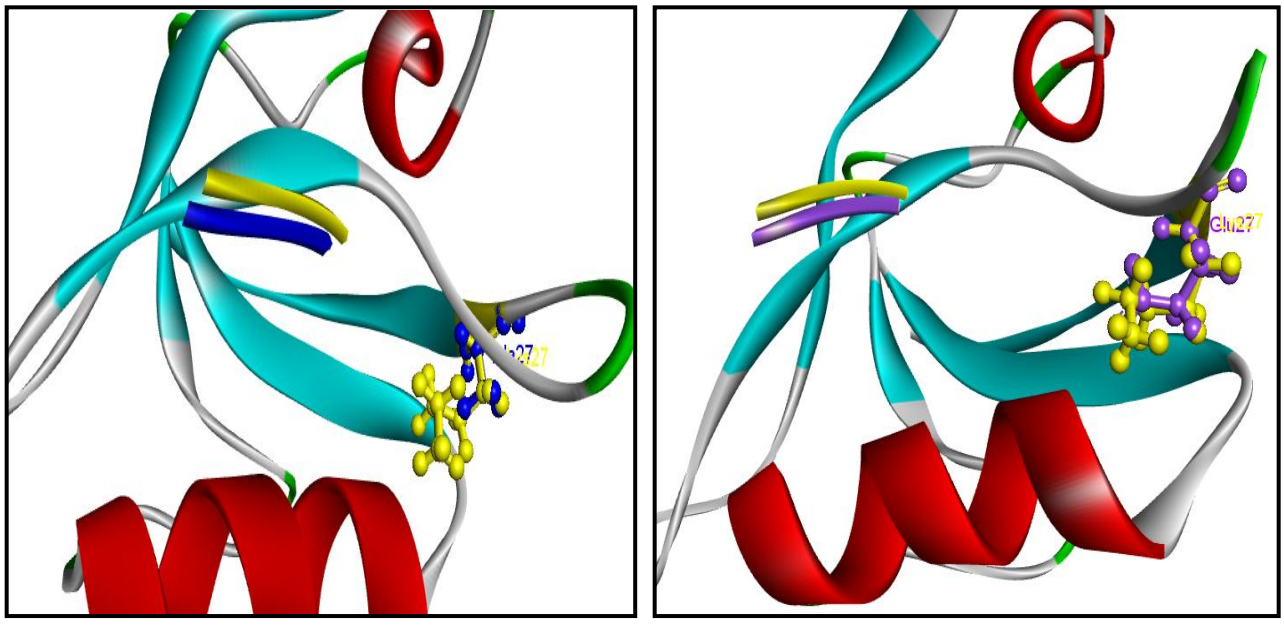

Figure 4-7 WT IPEV-PICK1 complex superimposed on the K27A (left) and K27E (right) mutant PICK1 complexes. The backbone structure does not deviate much (Backbone rmsd ~0.8 for both cases), but the peptide gets closer to the protein in the binding region compared to WT. K27 in the WT structure is shown in yellow, A27 is in blue and E27 in purple. Peptides in each complex are colored accordingly.

Another striking result is that even though Lys27 is a highly conserved residue, in all cases K27 mutants turn out to be better binders. One of the reasons for the decrease in the energy is the substitution of Lys itself, i.e it lowers the energy of the complex with its individual contribution compared to Ala or Glu. The second reason is that in most of the cases Lys causes unfavorable energy in the loop region it lies. Structures of K27 mutants of IPEV, Type II complex with the largest energy difference between the WT and K27 mutants, are demonstrated to represent this behavior commonly exhibited by most of the complexes (Figure 4-7). K27 mutations do not alter the backbone geometry much (Backbone rmsd of ~ 0.8 ± 0.2 for all cases) rather the position of the peptide changes getting closer to the binding pocket. K27A complexes involves in less interaction yielding lower binding energies than both WT and K27E for most of the complexes due to the smaller side chain.

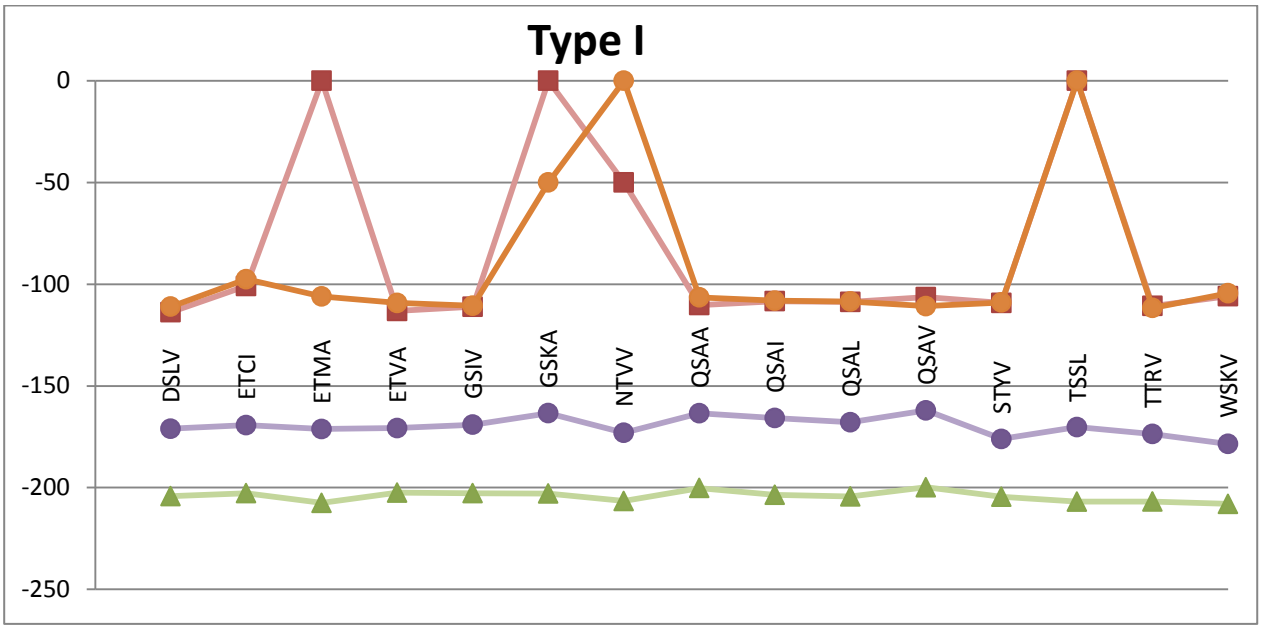

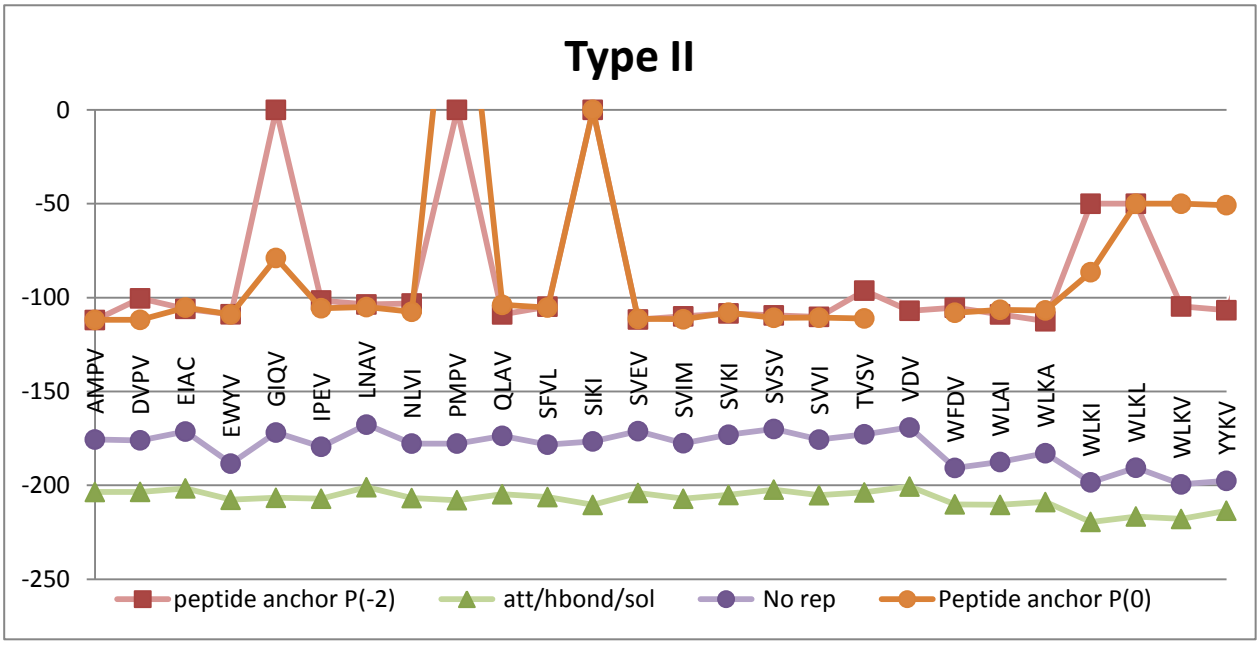

Figure 4-8 FlexPepDock protocol is repeated with different scoring schemes and with different peptide anchors (P(0) and P(-2), using standard scoring function). Both omiting only the repulsive term (No rep) and combination of only the attractive, H-bond and solvation terms (att/hbond/sol) lowers binding energies and eliminates the unlikely positive scores. (All positive scores are represented as 0) Use of P(0) as anchor instead of P(-2) avoids high scores of ETMA, GIQV, PMPV but does not cause any meaningful change in general. (Data in Appendix Table 5-7)

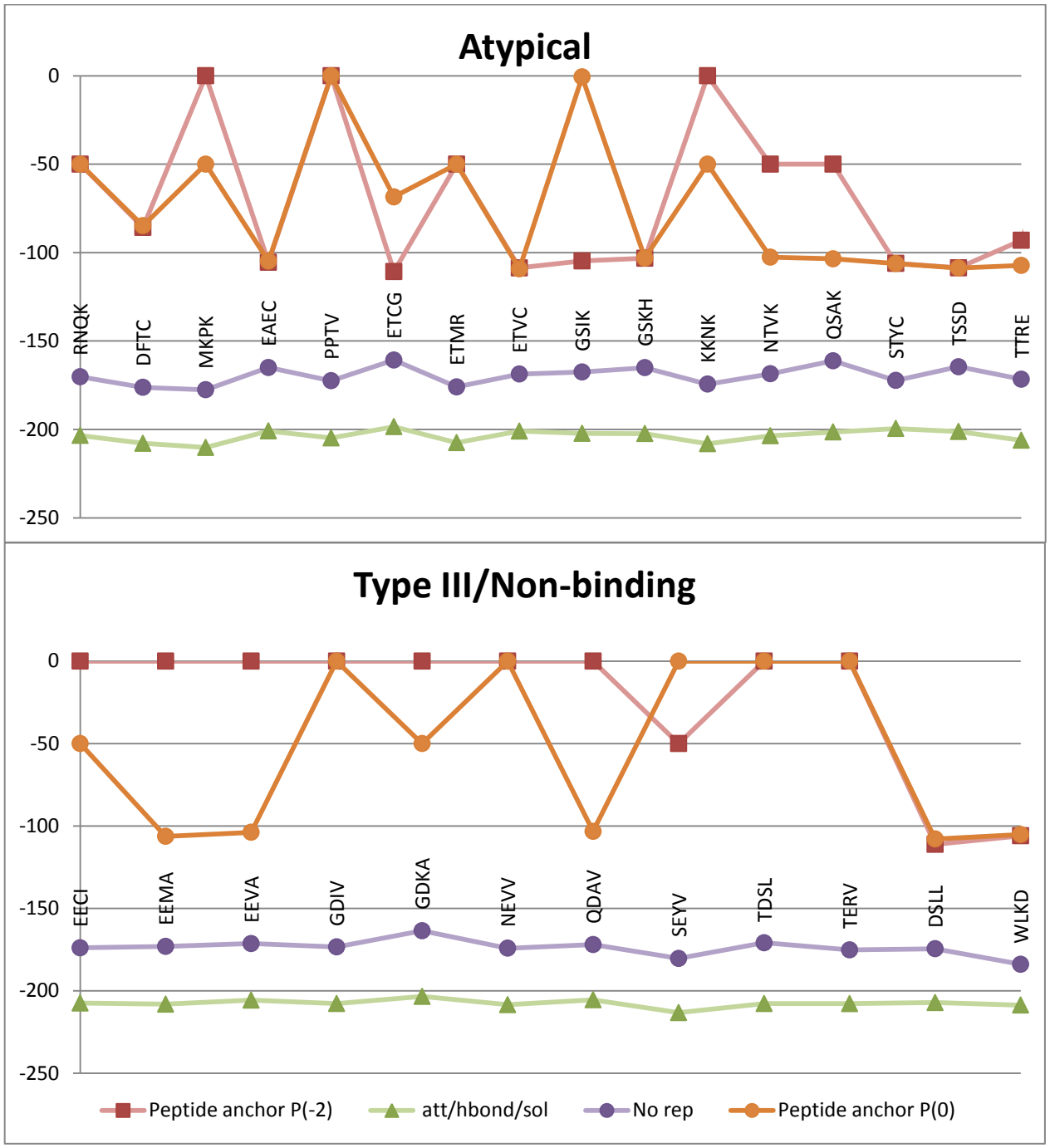

Figure 4-9 (Continued from Figure 4-8) Effect of change of parameters for Atypical, Type III and Non-binding peptides. The contribution of the repulsive term is evident for these groups of peptides than it is for Type I and II. Still some peptides are recovered from unlikely high scores by use of P(0) as anchor. (Data in Appendix Table 5-9)

FlexPepDock experiments are repeated with different parameters, changing the scoring function and setting different anchor residues, to see if the results could be improved (Figure 4-8, 4-9). From the previous runs repulsive term in the energy function is detected as the biggest contributer to the Total Score resulting in unlikely positive energy values. Thus, complexes are evaluated with the repulsive term dropped as the first alternative scheme and with the combination of only attractive, h-bond and solvation energy terms as the second. Compared to the standard scoring function these schemes eliminate the high scores as expected. Yet, there is no considerable difference between the two schemes demonstrating the dominance of the repulsive term once again. Upon elimination of the repulsive term, peptides with amino acids W (Tryptophan) and Y (Tyrosine) looks more favored.

Choice of peptide anchor is another parameter that is experimented with. Commonly in the binding process of partner peptides to the PDZ protein, P(0) residue, located in the C-ter of the peptide, interacts with the carboxylate binding loop of the protein regardless of the interaction type. P(-2) residue on the other hand is the determining residue of the PDZ type. Thus to see the effect of these interactions, two runs are carried out with each residue set as the anchor under the standard scoring function. Since the repulsive term dominates in the standard scoring function complexes turn out to have positive scores. Still, use of P(0) as anchor recovered 3 out of 7 complexes, namely ETMA, GIQV, PMPV, WLKI among Type I and II. However, different anchors do not alter the results for Atypical and Non-binding groups including Type IIIs.

4.2 PepCrawler

PepCrawler is tested for several groups of proteins like MH Class Is, SH3 domains, and also PDZ domain proteins where it showed a performance poorer than the other two groups yet still considerable. The relatively short length of the peptides is pointed out as the cause of the lower performance[5].

After initial PICK1-peptide complexes are freed of intermolecular clashes using ClassicRelax routine of Rosetta, they are fed into PepCrawler algorithm. Resultant minimum energy complexes are represented as classified according to their PDZ Type (Figure 4-10). When the score of non-binding peptide DSLL is again set as the boundary, more of the known binding peptides scores lie above it. Also, Type III peptides, initially assumed as non-binders, are scattered and there is no apparent separation of binding and non-binding peptides. Yet, Type II peptides score relatively better compared to other types and atypical complexes tend to have high binding energies. Amino acids Serine, Trytophan and Tyrosine are more likely to occur among peptides with most favorable energies, still known non-binder WLKD peptide's complex scores relatively lower. Complexes with peptides bearing a Proline residue are not present on the plot since PepCrawler did not converge for these complexes.

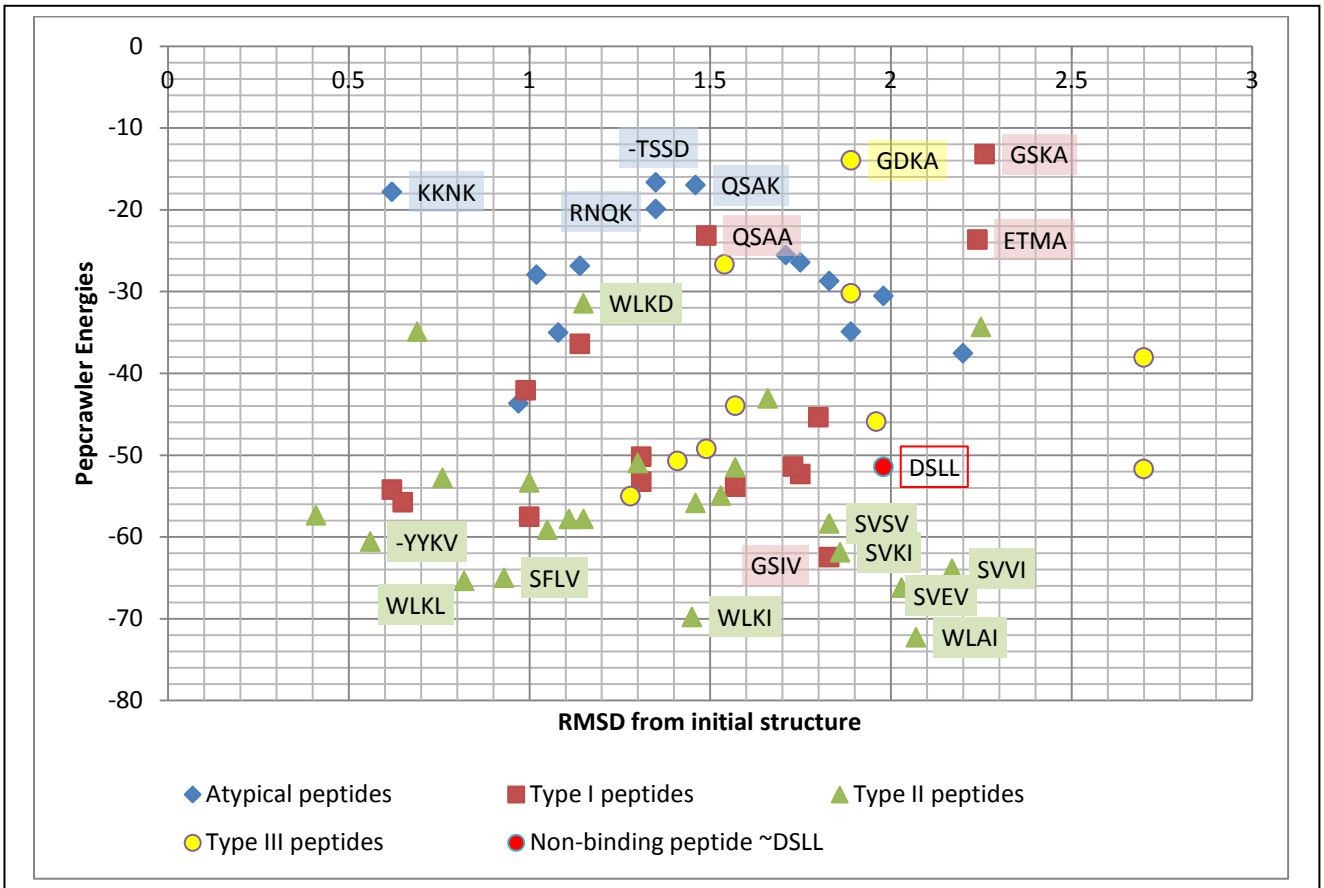

Figure 4-10 Distribution of the energies of the Type I, II, III and Atypical peptide complexes calculated with PepCrawler. Each point on the plot corresponds to the complex of PICK1 with a peptide as listed in Table 3-1. (Complete data available in Appendix Table 5-8)

Similar to the analysis done with FlexPepDock, K27A, K27E, K83H and K83V mutant complexes are evaluated with PepCrawler (Figure 4-11). Based on these calculations, both Type I and Type II complexes showed increased binding energies upon K27 mutation. Though KD motif is conserved in Type II, its contribution in the Carboxylate binding loop makes this residue important for both types since PDZ domain binds C-termini peptides. More specifically K27E looks more disruptive than the K27A. Regarding the K83 mutations, the complexes tend to have lower energies implying higher binding affinities. In 12 out of 16 Type II complexes K83V mutants have shown lower energies compared to K83H which supports the conventional type-specific preferences of αβ1 position.

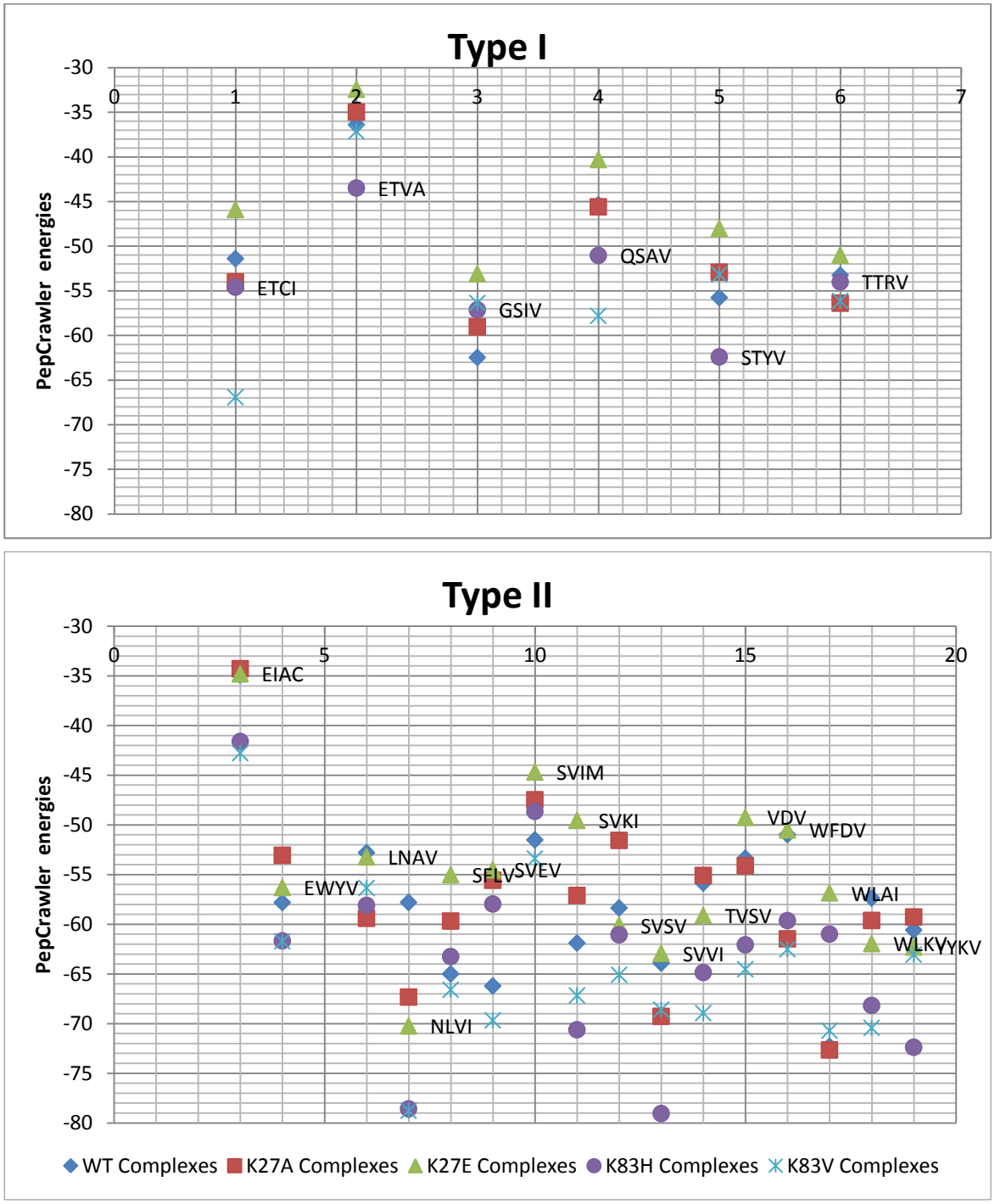

Figure 4-11 Minimum energies sampled by PepCrawler of PICK1 PDZ domain WT and K27A, K27E, K83H and K83V mutant-Type I and Type II peptide complexes (Data available in Appendix Table 5-4)

4.3 X-Score

The resultant structures from FlexPepDock process are re-evaluated using another scoring function X-Score for further comparison. In this way, the energy distribution of the same complexes is investigated to see if they exhibit same trends or not under a knowledge-based scoring scheme. This analysis is carried out using the Predicted binding energies and Predicted binding affinities produced with X-Score for both WT and mutated complexes in the dataset.

Analysis reveals that there is not a remarkable distinction observed between binding and non-binding peptides in the distribution of the X-Score energies of the complexes. Taking the non-binding peptides DSSL and WLKD as reference points again, no clear preference of binders over non-binders is exhibited. Yet, Type III complexes perform higher binding energies as expected as well as Type II peptides tend to have lower energies (Figures 4-12, 4-13). Another point is that peptides bearing Tryptophan (W), Tyrosine (Y) are favored over the others. A closer look on these complexes reveals the atoms of the aromatic side chains contributes most to the total energy score. Since the scores are calculated as the sum of per atom contribution, Van der Waals term dominates for these complexes which might create a bias. Concerning the highest binding energy complexes, it performed poorly by placing some of the known binding partners in this group.

Carrying out the same analysis as done with the other two tools, mutant complexes are also evaluated with XScore (Figure 4-14). Upon mutation predicted binding energies of the complexes do not change remarkably. Decreased binding energy of the K27 mutant complexes and the increase in the K83 complexes compared to the WTs is the second result to stand out as contrary to the findings of the PepCrawler. Not surprisingly, energy values calculated with XScore matches the trend found by FlexPepDock. Still no type specific behavior is observed.

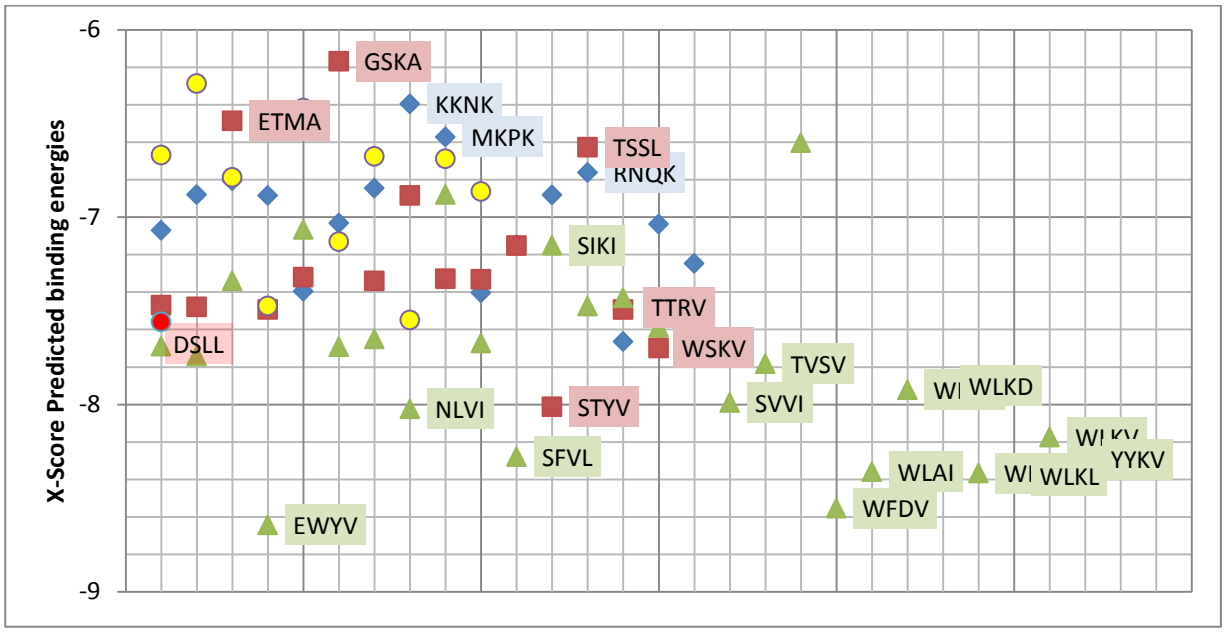

Figure 4-12 Distribution of the binding energies of the complexes calculated with X-Score (Data available in Appendix Table 5-8)

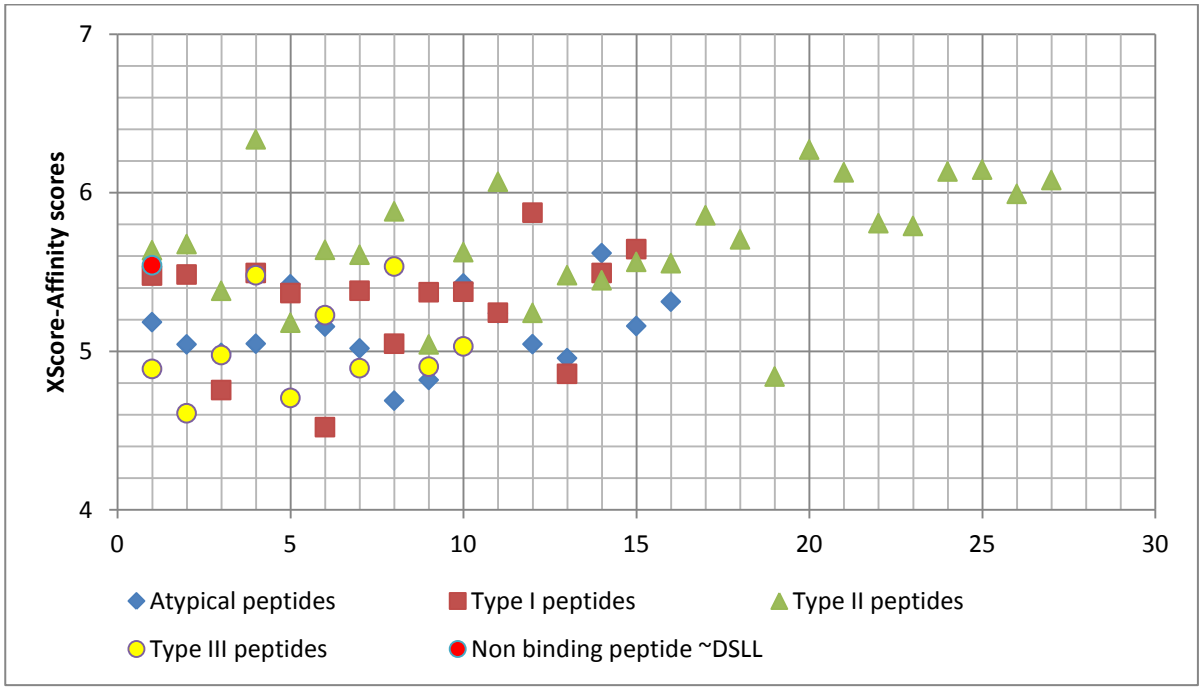

Figure 4-13 X-Score Predicted Binding Affinity scores of the complexes ($logK_D$). (Peptides are indexed on the x-axis as listed in Table 3-1)

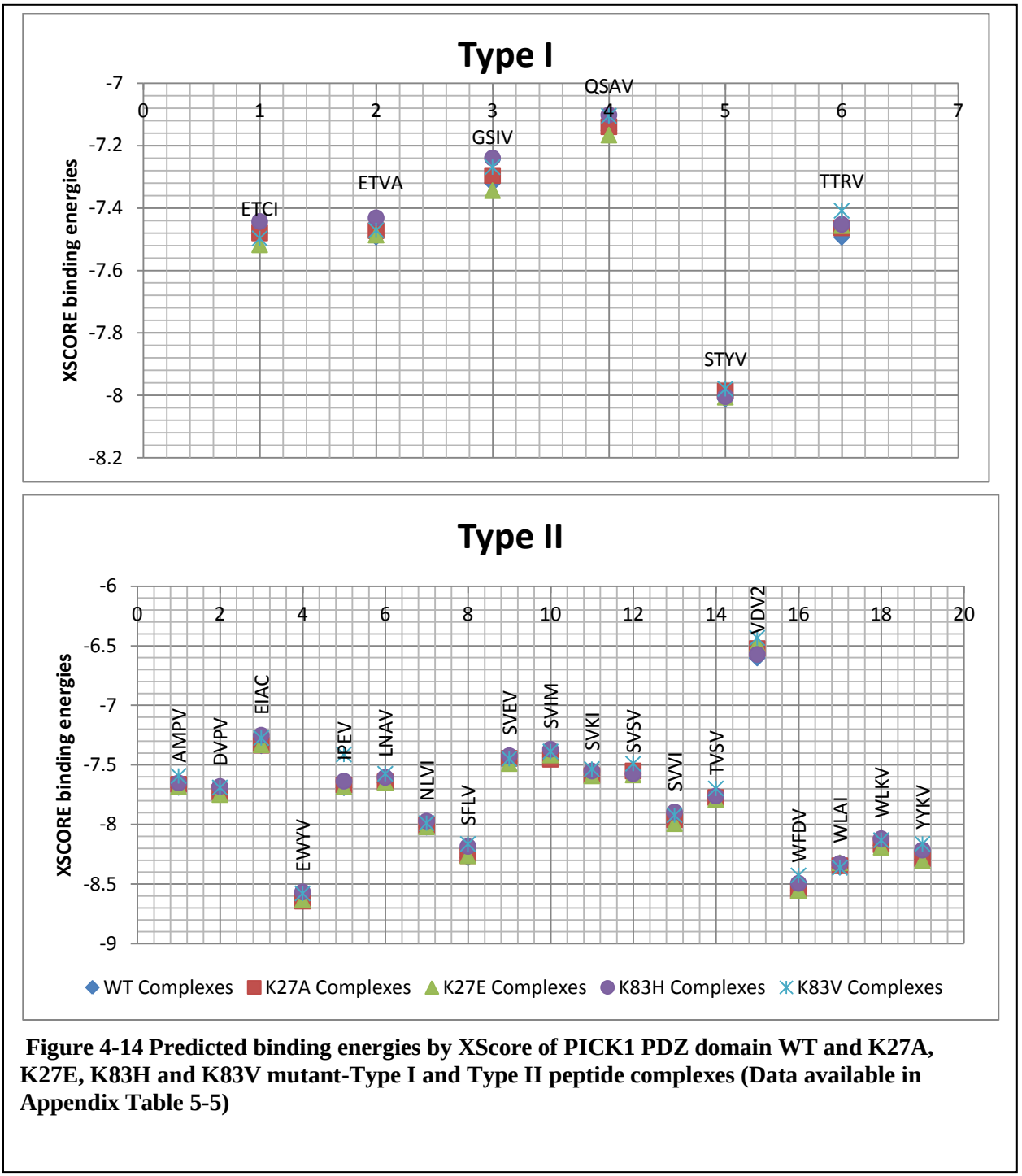

Figure 4-14 Predicted binding energies by XScore of PICK1 PDZ domain WT and K27A, K27E, K83H and K83V mutant-Type I and Type II peptide complexes (Data available in Appendix Table 5-5)

4.4 Comparison of the Scoring Tools

Due to the differences in the scoring functions, it is not possible to compare the binding energies calculated with each protocol quantitatively. Each protocol incorporated the energetic terms with different weights yielding values spanning different ranges. Thus, an assessment can be carried out by comparing extend of the agreement with the established knowledge and the prediction performance of each tool regarding PICK1 PDZ-peptide binding.

To start with, in discriminating the binding and the non-binding peptides, all three tools place the artificial complexes with presumably non-binding Type III peptides among the lowest scored ones (Figures 4-3, 4-10, 4-12). Yet, FlexPepDock performs better over the other two tools by placing smaller number of binding peptides in the same range as the non-binding ones. PepCrawler and X-Score did not put out a distinction between the binding and non-binding peptides as clear as FlexPepDock did. Moreover, they position all atypical peptides together with the Type IIIs, both experimentally identified binding peptides and artificially generated ones. On the other hand, all three tools favored Type II peptides over the other types supporting higher preference of PICK1 PDZ domain for Type II peptides. However, there is less agreement concerning the high scoring peptides (Table 4-2). Even though X-Score calculations are carried out with the structures obtained from FlexPepDock protocol, they resemble more the PepCrawler results regarding the ranking of the complexes based on the binding energies. Both PepCrawler and X-Score identify the complexes of the same peptides as the ones with lowest binding energies whereas FlexPepDock differs from the two placing those peptides lower in the ranking. Based on this comparison, peptides with Tryptophan (W) or Tyrosine (Y) seem favored according to PepCrawler and X-Score. Complexes with the lowest binding affinities are more shared between the three functions than the top scoring complexes are (Table 4-3). (Refer to the Appendix Table 5-8 for the complete list)

PepCrawler performed better than the other two in reflecting the trend that Type I and Type II peptides follow as regards the mutational analysis, involving the K27 and K83

PICK1 mutants. Though not discriminating between Type I and II, it finds K27 mutations disturbing and K83 mutations favoring the binding. Yet FlexPepDock unexpectedly finds K27 mutations enhancing the binding and K83 mutations disrupting it for most of the complexes regardless of the peptide Type. Sure enough this trend is also exhibited by X-Score (Figures 4-6, 4-11, 4-14).

Table 4-1 Top 10 Highest scoring complexes based on the binding energies

FlexPepDock		PepCrawler		X-Score	
ETVA	-112,227	WLAI	-72,28	EWYV	-8,6431
AMPV	-111,392	WLKI	-69,8	WFDV	-8,5538
QSAA	-110,316	SVEV	-66,21	WLKL	-8,3818
QSAV	-109,581	WLKL	-65,38	WLKI	-8,3663
ETVC	-109,238	SFLV	-65	WLAI	-8,3589
TVSV	-108,787	SVVI	-63,91	YYKV	-8,293
STYC	-108,352	GSIV	-62,48	SFLV	-8,2788
SVSV	-108,336	SVKI	-61,89	WLKV	-8,1746
ETCG	-108,263	YYKV	-60,58	NLVI	-8,0234
TSSD	-108,171	SIKI	-59,13	STYV	-8,0123

*Complete data can be found in Appendix

Table 4-2 10 Lowest scoring complexes based on the binding energies

FlexPepDock		PepCrawler		X-Score	
TDSL	-28,5521	TTRE	-26,44	QDAV	-6,6759
TSSL	-27,3073	ETCG	-25,54	EECI	-6,6688
GDIV	-24,5791	ETMA	-23,65	TSSL	-6,6269
EECI	-18,8814	QSAA	-23,16	VDV2	-6,603
SIKI	-18,0724	RNQK	-19,91	MKPK	-6,5724
NTVV	-17,5168	KKNK	-17,82	ETMA	-6,4861
TERV	-13,8444	QSAK	-16,99	GDKA	-6,4182
NEVV	-11,1379	TSSD	-16,65	KKNK	-6,3958
DFTC	13,5544	GDKA	-13,96	EEMA	-6,2871
VDV	55,1194	GSKA	-13,2	GSKA	-6,1682

4.5 Comparison with the Experimental Data

In order to see if the energy calculations actually have predictive power, the results are compared with the experimental data available in literature.

In the Madsen et al 2005 paper, binding affinity of PICK1 for its Type I and Type II peptides is studied with a binding assay based on fluorescence polarization (FP) [33]. 13 residues long C-termini peptides from Protein Kinase Ca (~QSAV) as Type I, DopAmine Transporter (~WLKV) as Type II and (~DSSL) as non-binding control peptide was used. Additionally, mutations were introduced both on PICK1 (K83V, K83H) and on the P(0) and P(-2) position of peptides. Complexes and corresponding binding affinities from this work are compared with the PepCrawler, XScore and FlexPepDock scores.

FP data comprise of K_i values, dissociation constant of the PICK1- peptide complexes, in units of μM, i.e. the higher the K_i, the lower the binding affinity. It is not possible to compare this data with the binding energies calculated with any of the scoring functions used in this study. Therefore, the results are compared qualitatively by analyzing the binding behavior of PICK1 towards different peptides and upon different mutations. Overall FlexPepDock is found to represent the experimental data better than the other two. (Figure 4-15) In the broadest sense, none of tools stands out in reproducing the experimental findings based on the change in the energy scores. Though partial agreement between the FP data and each of the tools for different complexes, the general trend it exhibits cannot be completely reflected by any of them (Figure 4-16).

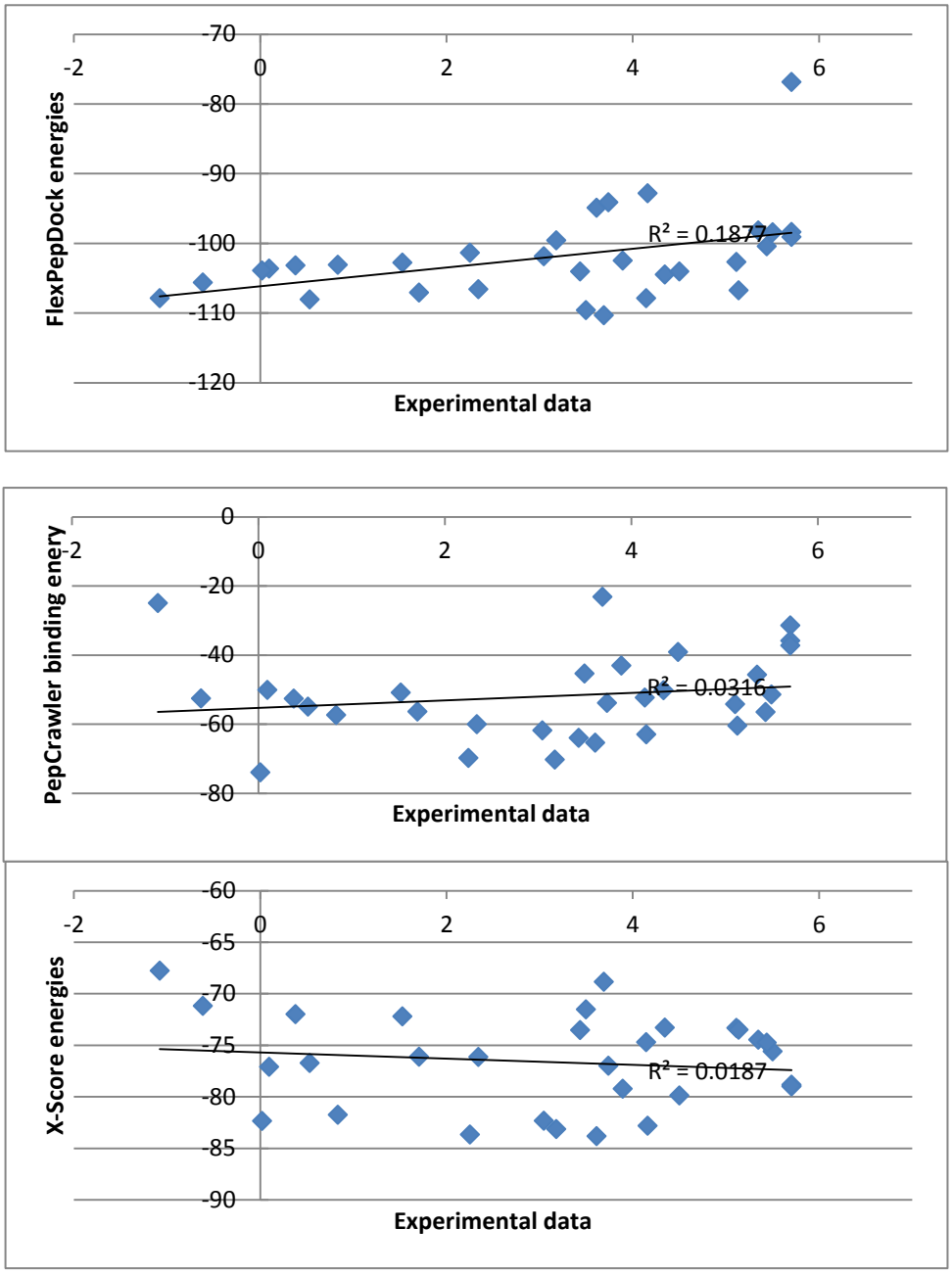

Figure 4-15 Comparison of the tools representativeness of the experimental data. FlexPepDock correlates the best among the three scoring schemes. Experimental data is represented on the abscissa in the form of $\ln(K_i)$(dissociation constant), higher values meaning lower affinity. Ordinates represent the binding energies calculated with the three different tools. No quantitative comparison is aimed in this analysis, figures are provided to make a comparison among the tools in representing the trend revealed by the experimental data. Experimental data is represented in logarithmic trend, since the relation between the binding energy (ΔG) and K_i is logarithmic. ($\Delta G = -RT\ln K_i$)

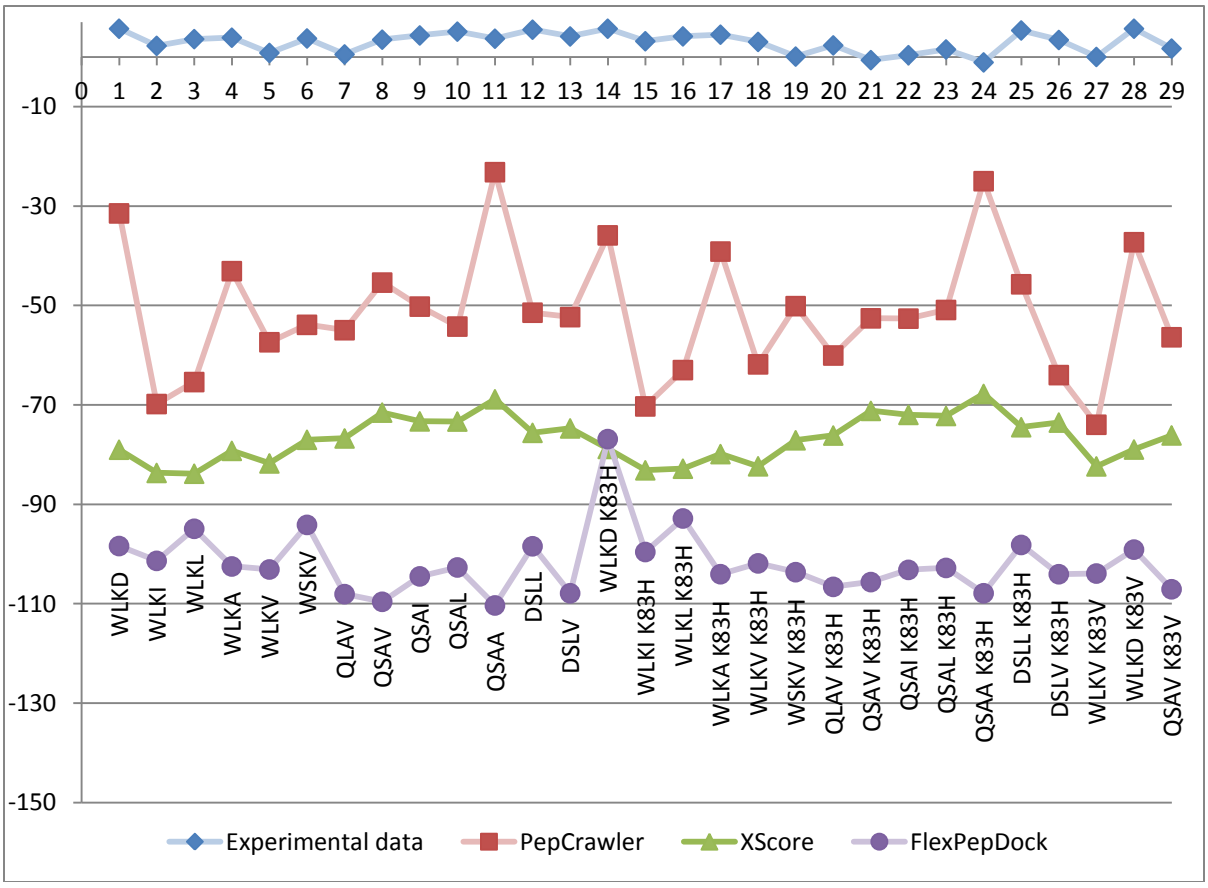

Figure 4-16 Comparison of the results of X-Score, FlexPepDock and PepCrawler with the experimental data. (For the scoring functions values are the energies of the complexes and experimental data is ln (K_i) (dissociation constant), meaning for all curves higher values imply lower binding affinities. (same for Figures 4-17, 18, 19, 20, 21) In order for the values fall in the same range, X-Score energies are multiplied with 10. Also K_i values of >1000 are evaluated as 300 to keep the graph in proper scale) (Complete data available in Appendix Table 5-6)

When it comes to more specific comparisons preference for Type II peptide over Type I is represented by PepCrawler and X-Score. However, this might be due to these functions favoring the complexes with peptides carrying a W, rather than discriminating between Type I and II. Regarding the change in binding affinities upon different amino acids in P(0), FlexPepDock predicts the behavior of Type I peptide (~QSAV) more successfully than PepCrawler and XScore (Figure 4-17). Experimental data suggests a preference Val> Ile> Leu for the P(0). Though FlexPepDock reproduces this ranking for both peptides, PepCrawler performs better in predicting the behavior of the Type II peptide (~WLKV) upon

mutations than the other two tools (Figure 4-18). Preference for Val in the P(0) position over Leu is confirmed by all three tools regardless of the mutation on PICK1 in case of non-binding peptide ~DSLL. (Figure 4-19) The preference order Val> Ile> Leu also holds true for the K83H mutant PICK1s in complex with Type I and II peptides with varying P(0) (Figure 4-21). Even though the experimental data disfavors Ala in P(0) only in Type II, it is found to be disfavored in both types by FlexPepDock. This might be due to the decreasing number of contacts Ala makes with P(0) binding pocket residues compared to Val, Ile and Leu which might make the complex less stabilized. Also, the elimination of the interaction when P(0) is mutated to negatively charged Aspartate is revealed by all three functions.

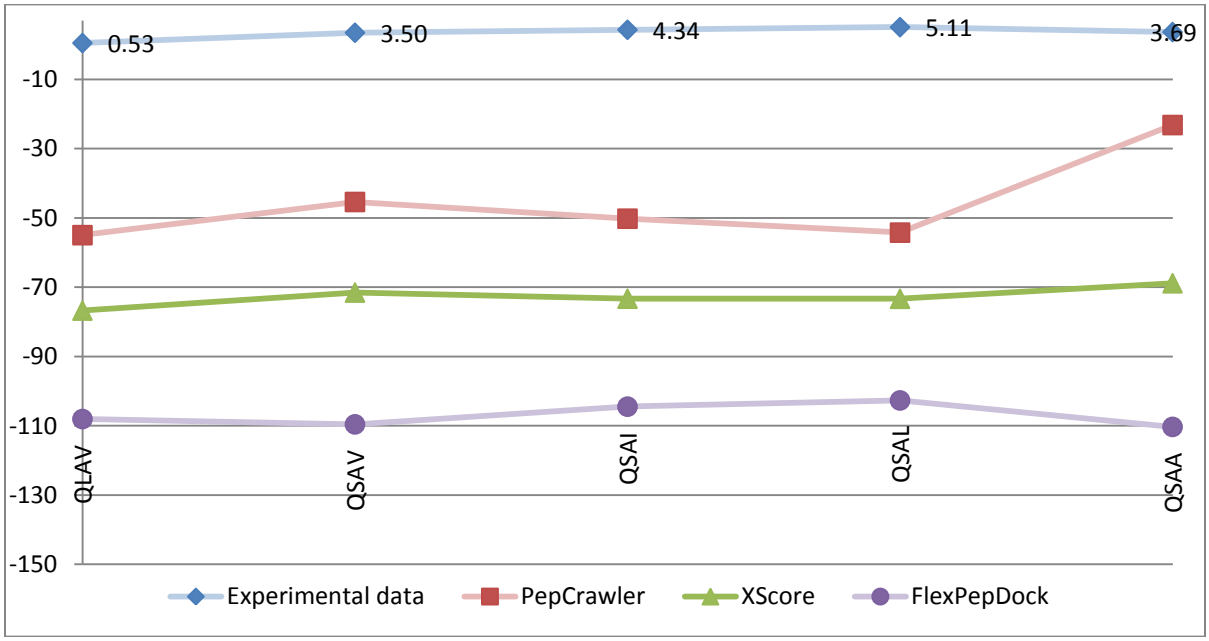

Figure 4-17 Binding energies of the ~QSAV peptide and its mutants

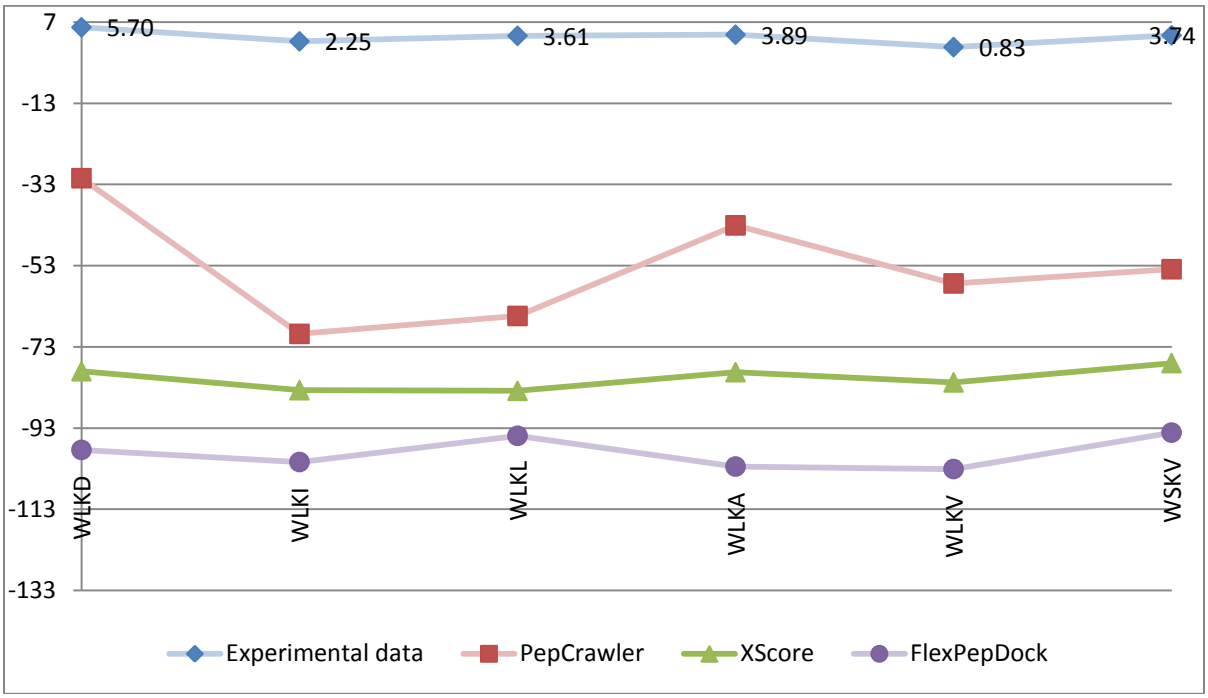

Figure 4-18 Comparison of the binding energies of the ~WLKV peptide and its mutants

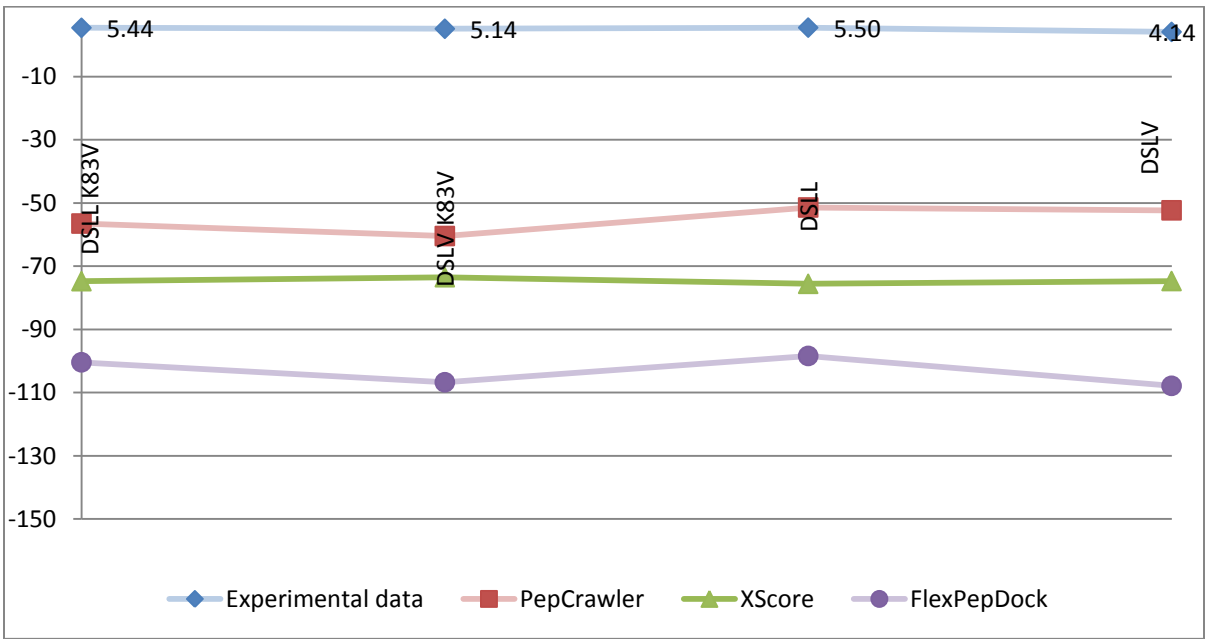

Figure 4-19 Comparison of the binding energies of the ~DSLL peptide and its mutants

Concerning another set of analysis carried out in the experimental work, binding affinities of the mutant Type I and Type II peptides for the investigation of the P(-2) residue of the peptide are reflected better by PepCrawler. However it cannot present the same

performance with the K83H complexes of the same peptides (Figure 4-20, 4-21). For this part of the analysis, none of the tools produce results in agreement with the experimental findings.

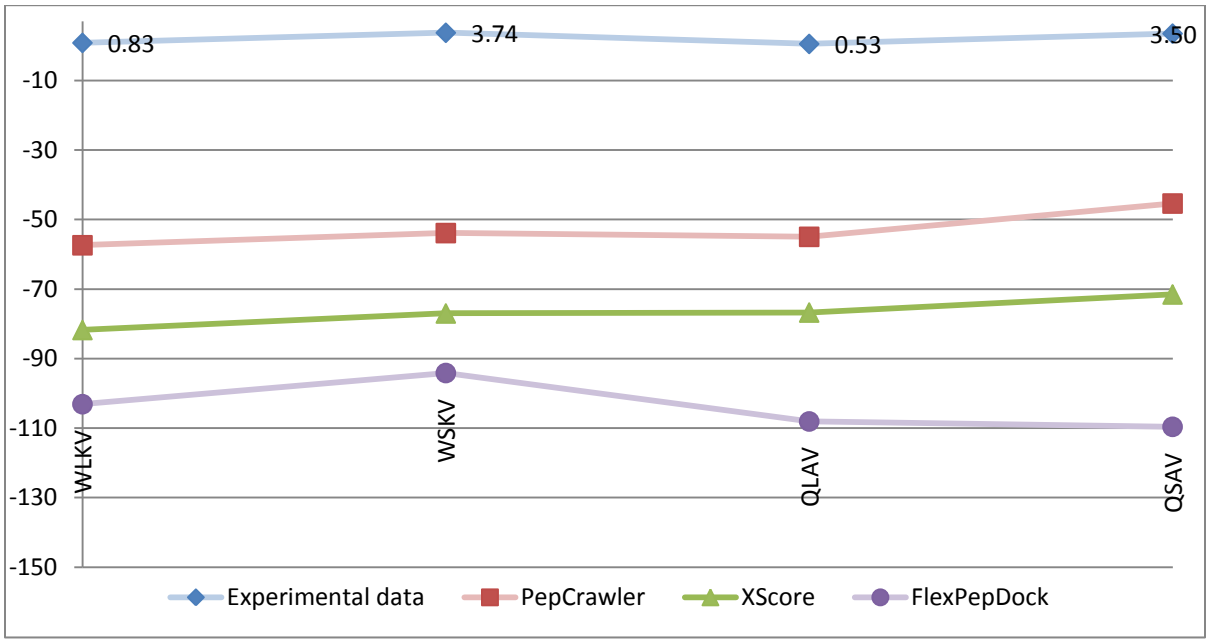

Figure 4-20 Comparison of the experimental data regarding the effect of P(-2) residue on Type I and Type II peptides with FlexPepDock, PepCrawler and X-Score

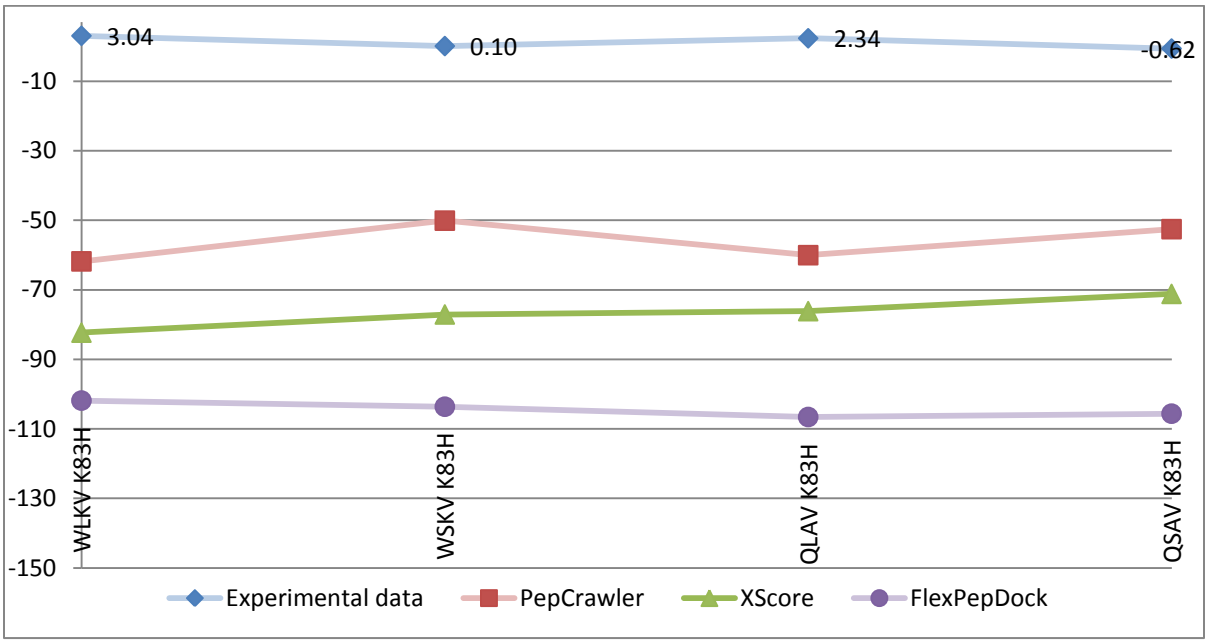

Figure 4-21 Experimental data of K83H complexes with Type I and Type II peptides and their mutants in comparison with FlexPepDock, PepCrawler and X-Score output

Once FlexPepDock is found to perform better in representing the experimental data, runs are repeated with modifying several parameters, as mentioned above in Section 4.1. Two different energy schemes are tried, one with omitting the repulsive term and the second including only attractive, hbond and salvation terms, and compared with the standard energy function to see if they could better reflect the experimental findings. Apart from that, P(0) and P(-2) are set as peptide anchors as another parameter and compared if any of them could improve the prediction performance (Figure 4-22).

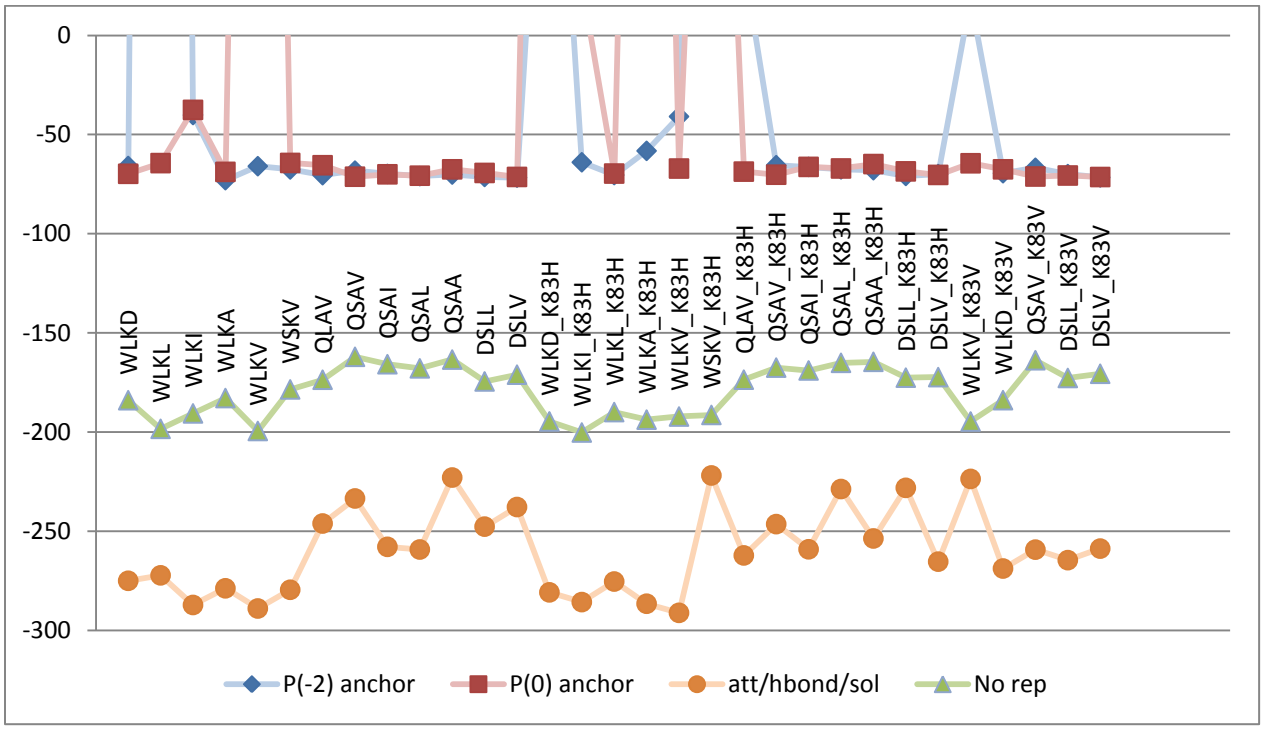

Figure 4-22 FlexPepDock scores under two different energy schemes and in cases where P(0) an P(-2) are set as anchors. (Data available in Appendix Table 5-9)

Chapter 5
CONCLUSION

PICK1's role in nervous system and many related diseases becomes more and more established with the accumulating evidence by recent research. Carrying out many of its interactions through its single PDZ domain, knowledge on the binding behavior of this curious protein should sure to contribute many of the related studies including not only PICK1 but also PDZ domains and evaluation of protein-peptide complexes in general.

This study takes advantage of the available computational tools to investigate the PDZ domain interactions of PICK1. Two different protein-peptide complex assessment tools, FlexPepDock and PepCrawler, are experimented with 69 PICK1-peptide complexes including members from all three PDZ types (Type I, II and III), atypical peptides and experimentally determined non-binders. In order to see the binding trends exhibited under a differet scoring scheme, PICK1–peptide complexes are evaluated with yet another scoring function, X-Score. Performances of these tools are evaluated in comparison with each other and with the available experimental data. General tendency of PICK1 for Type II partners is captured by all three tools. PICK1's lack of any known Type III partners is also reflected by all three tools placing these complexes as the lowest scoring ones. Additionally, PepCrawler scores of the atypical peptides shows a disfavor for these complexes.

Concerning more specific comparisons, FlexPepDock emerged as the one with the best performance correlating with the experimental data higher than the other two. However, it did not carry this performance onto discrimination of K27 and K83 mutations. PepCrawler demonstrates the disruptive effect of K27 mutations and represents the binding trends upon K83 mutations better.

FlexPepDock protocol is experimented with changing the parameters like scoring schemes, various constraints and anchor residues to explore the capabilities of FlexPepDock and improve the performance further which is partly achieved with using a different scoring

scheme which excludes the repulsive contribution. However, upon each modification there are correctly predicted behaviors as well as the ones which could not be identified. Upon increase in the experimental binding affinity data, improvement in the prediction performance of the tool and generation of a better scoring function would be possible.

Regarding future directions, current work might have implications for studies concerning identification of new PDZ partners for PICK1 as well as PDZ domain targeted drug discovery. Computational analysis could be extended with use of other parameters, different combination of energy terms to back up possible experimental studies. In a broader sense, it could also be utilized by research involving PDZ interactions and discussion of concepts related to assessment of protein-peptide complexes.

APPENDIX

Table 5-1 FlexPepDock output of the 69 PICK1-peptide complexes in the dataset

Peptide sequence	Total Score of the Minimum scoring decoy	Overall rmsd (initial structure to Minimum scoring decoy)	Backbone rmsd (initial structure to Minimum scoring decoy)	Backbone rmsd (averaged over 500 decoys)	Total score (Average of all 500 decoys)
DFTC	-102.381	4.336	4.527	4.05131	-85.5352
EAEC	-113.628	2.583	1.39	0.800094	-104.266
ETCG	-114.059	2.668	1.726	1.22046	-106.475
ETMR	-114.825	3.265	1.172	0.806742	-107.231
ETVC	-115.343	2.154	1	0.86574	-107.261
GSIK	-113.872	1.677	0.629	0.922958	-104.632
GSKH	-110.9	2.656	1.549	1.84353	-96.6225
KKNK	-109.712	6.979	6.947	4.02573	-64.5151
MKPK	-110.448	5.948	5.248	4.65609	-75.955
NTVK	-114.57	2.024	0.983	0.823296	-106.084
PPTV	-107.753	3.99	3.812	4.86396	-91.2184
QSAK	-116.145	2.365	0.593	0.761144	-105.412
RNQK	-114.781	3.214	1.144	0.794626	-102.116
STYC	-114.175	2.913	0.655	0.86743	-109.395
TSSD	-115.709	1.349	0.54	0.465862	-109.283
TTRE	-115.112	1.6	0.571	0.65446	-106.827
DSLV	-114.482	1.974	0.704	0.747804	-103.649
ETCI	-110.621	1.855	0.925	0.898218	-99.3701
ETMA	-109.297	6.103	5.738	2.74655	-86.2124
ETVA	-117.018	2.314	0.994	0.867884	-109.789
GSIV	-113.732	0.999	1.07	0.947554	-105.168
GSKA	-108.44	5.03	4.161	3.47757	-83.2154
NTVV	-109.852	3.991	3.641	4.50639	-80.7329
QSAA	-115.76	1.762	0.651	0.858732	-107.633
QSAI	-113.632	1.881	0.872	0.791796	-103.633
QSAL	-114.033	2.183	0.835	1.16938	-102.787
QSAV	-115.638	2.288	1.282	0.754604	-106.062
STYV	-115.003	2.957	0.913	0.786822	-109.24
TSSL	-111.775	7.013	6.86	3.98824	-56.1727

TTRV	-113.273	3.898	3.791	0.807166	-106.663
WSKV	-108.948	2.931	0.962	0.831252	-100.789
AMPV	-114.74	1.054	1.057	0.78793	-109.164
DVPV	-116.076	1.135	0.888	0.913366	-109.775
EIAC	-112.947	1.66	0.518	0.677072	-106.61
EWYV	-112.735	2.872	0.997	1.04045	-103.952
GIQV	-109.636	7.078	7.222	5.25802	-90.0678
IPEV	-112.585	2.989	2.208	1.20085	-105.709
LNAV	-110.837	0.758	0.574	0.699794	-105.118
NLVI	-113.714	0.968	0.569	0.659952	-107.379
PMPV	-108.1	4.039	3.433	4.68295	-71.5939
QLAV	-114.601	1.845	0.622	0.684864	-106.871
SFVL	-110.443	1.708	1.179	0.87814	-101.034
SIKI	-108.617	6.833	5.91	4.92751	-58.9537
SVEV	-114.791	1.226	0.913	0.684192	-107.569
SVIM	-112.33	1.424	0.843	0.736286	-103.808
SVKI	-112.844	2.288	0.824	0.74038	-104.686
SVSV	-114.542	1.157	0.798	0.626468	-108.772
SVVI	-113.22	1.122	0.736	0.715324	-106.694
TVSV	-116.194	0.938	0.83	0.680898	-109.19
VDV	-112.089	2.006	1.998	0.955954	-96.4168
WFDV	-111.974	2.292	0.626	0.821762	-100.9
WLAI	-114.376	2.044	0.53	0.71422	-102.394
WLKA	-115.563	1.991	1.298	0.661582	-99.4755
WLKD	-112.208	2.191	0.411	0.625394	-100.292
WLKI	-113.17	3.522	1.028	0.807672	-96.0556
WLKL	-110.591	3.14	0.783	1.00894	-102.044
WLKV	-114.106	3.55	1.429	0.685556	-100.077
YYKV	-114.643	3.3	1.058	0.846952	-103.042
EECI	-109.301	5.985	5.715	4.5238	-64.9066
EEMA	-111.809	5.161	4.326	3.04439	-86.0371
EEVA	-109.263	5.001	4.393	3.67425	-65.9289
GDIV	-110.093	4.92	5.006	5.20668	-93.7119
GDKA	-110.193	6.349	5.978	3.52054	-80.652
NEVV	-108.436	4.869	4.777	4.56823	-76.7966
QDAV	-111.583	4.147	3.811	4.38612	-91.6193

SEYV	-110.427	5.697	4.379	4.43912	-73.2977
TDSL	-111.624	8.017	7.878	4.05521	-54.9603
TERV	-109.993	5.641	4.485	4.48059	-86.0892
DSLL	-112.312	3.475	3.053	1.24202	-102.045

Table 5-2 FlexPepDock scores under different sets of constraints

Peptide sequence	**Type**	**Total score (Averaged over all 500 decoys)**			
		Constraint I	Constraint II	Constraint III	Constraint IV
DFTC	A	-21.913	-53.9166	-83.7129	13.5544
EAEC	A	-106.972	-105.134	-105.598	-107.629
ETCG	A	-106.545	-106.811	-108.389	-108.263
ETMR	A	-106.71	-106.435	-106.516	-104.549
ETVC	A	-106.752	-107.22	-106.765	-109.238
GSIK	A	-104.547	-105.045	-105.143	-105.055
GSKH	A	-95.3114	-97.573	-94.4067	-95.1494
KKNK	A	180.057	34.8062	-71.8751	-61.2344
MKPK	A	271.501	78.9534	-91.0009	-50.0327
NTVK	A	-104.878	-106.105	-106.946	-104.958
PPTV	A	180.914	81.8196	-79.118	-49.8485
QSAK	A	-102.499	-106.527	-106.85	-105.394
RNQK	A	-102.255	-100.399	-102.054	-103.296
STYC	A	-108.205	-109.332	-109.194	-108.352
TSSD	A	-108.207	-108.732	-108.306	-108.171
TTRE	A	-107.449	-106.357	-106.666	-104.208
DSLV	I	-104.793	-103.585	-104.581	-107.869
ETCI	I	-100.222	-99.8116	-99.1704	-99.5578
ETMA	I	82.4493	-60.4106	-93.6526	-44.6773
ETVA	I	-109.277	-109.491	-110.04	-112.227
GSIV	I	-105.419	-104.455	-106.634	-107.644
GSKA	I	-52.8879	-82.2005	-91.879	-73.2198
NTVV	I	263.06	-1.74456	-87.0246	-17.5168
QSAA	I	-107.932	-107.795	-107.66	-110.316
QSAI	I	-104.324	-105.038	-104.179	-104.471
QSAL	I	-104.137	-102.422	-102.795	-102.672

QSAV	I	-108.05	-108.076	-108	-109.581
STYV	I	-108.102	-109.556	-110.3	-107.689
TSSL	I	-32.588	-30.8822	-83.8825	-27.3073
TTRV	I	-106.15	-105.676	-107.472	-106.294
WSKV	I	-93.4157	-93.5785	-94.6572	
AMPV	II	-110.411	-109.588	-110.081	-111.392
DVPV	II	-109.242	-109.89	-110.369	-108.094
EIAC	II	-106.07	-106.185	-107.748	-107.028
EWYV	II	-103.276	-104.501	-105.053	-105.993
GIQV	II	90.5911	23.13	-88.7431	-55.1745
IPEV	II	-104.681	-103.119	-105.911	-103.964
LNAV	II	-103.066	-105.485	-106.646	-106.209
NLVI	II	-107.657	-107.111	-106.677	-106.466
PMPV	II	445.47	111.204	-92.2335	-52.4265
QLAV	II	-101.621	-107.52	-107.499	-108.045
SFVL	II	-100.809	-99.3935	-100.365	-99.9782
SIKI	II	71.9269	-33.0517	-91.8809	-18.0724
SVEV	II	-107.198	-107.659	-108.305	-105.849
SVIM	II	-103.664	-105.008	-103.124	-102.316
SVKI	II	-104.923	-105.306	-104.398	-101.986
SVSV	II	-110.095	-110.655	-109.139	-108.336
SVVI	II	-106.436	-107.57	-106.078	-105.643
TVSV	II	-110.47	-110.192	-110.573	-108.787
VDV	II	7.0266	-76.1334	-104.009	55.1194
WFDV	II	-93.9513	-96.5628	-96.834	-98.5571
WLAI	II	-100.441	-102.361	-100.869	-99.5766
WLKA	II	-100.257	-101.087	-103.553	-102.473
WLKD	II	-97.8733	-99.415	-100.916	-98.369
WLKI	II	-99.1207	-100.223	-101.081	-101.351
WLKL	II	-93.8886	-97.4895	-96.307	-94.896
WLKV	II	-100.552	-101.027	-102.619	
YYKV	II	-98.8688	-98.138	-100.203	
EECI	III	63.1891	15.0882	-82.2391	-18.8814
EEMA	III	34.6254	-65.6461	-89.5082	-51.7932
EEVA	III	64.2091	-51.0102	-93.1724	-33.8158
GDIV	III	83.7533	75.2487	-74.5858	-24.5791

GDKA	III	-56.0741	-66.7746	-93.5941	-55.0677
NEVV	III	51.1671	31.6297	-64.6468	-11.1379
QDAV	III	77.6833	52.5566	-89.2938	-46.9867
SEYV	III	33.1075	53.8162	-68.87	-60.5019
TDSL	III	50.7474	-47.4966	-79.2962	-28.5521
TERV	III	31.2004	-33.8017	-81.3175	-13.8444
DSLL	N	-100.806	-100.441	-101.52	-98.4145

Table 5-3 FlexPepDock scores of a subset of 27 Wild Type and mutant PICK1-peptide complexes

Peptide sequence	**Type**	**Total score (Averaged over all 500 decoys)**				
		WT	K27A	K27E	K83H	K83V
EAEC	A	-107.629	-109.162	-109.052	-104.784	-106.046
RNQK	A	-103.296	-104.018	-104.143	-102.337	-101.394
ETCI	I	-99.5578	-101.96	-105.517	-102.644	-103.02
ETVA	I	-112.227	-114.84	-114.529	-112.048	-111.648
GSIV	I	-107.644	-110.205	-110.066	-106.077	-107.567
QSAV	I	-109.581	-103.517	-110.479	-105.274	-107.723
STYV	I	-107.689	-109.093	-109.892	-106.282	-107.102
TTRV	I	-106.294	-108.526	-108.938	-103.868	-107.805
AMPV	II	-111.392	-109.035	-113.41	-109.965	-110.337
DVPV	II	-108.094	-111.006	-110.249	-107.28	-108.215
EIAC	II	-107.028	-109.748	-107.609	-106.155	-106.947
EWYV	II	-105.993	-108.662	-108.487	-99.871	-105.913
IPEV	II	-103.964	-106.459	-105.909	-102.638	-94.1
LNAV	II	-106.209	-107.932	-111.347	-109.156	-107.718
NLVI	II	-106.466	-109.984	-107.62	-106.452	-106.977
SFLV	II	-99.9782	-105.627	-106.406	-100.271	-103.358
SVEV	II	-105.849	-108.373	-104.496	-105.971	-105.764
SVIM	II	-102.316	-102.924	-106.503	-102.208	-104.414
SVKI	II	-101.986	-105.472	-106.05	-103.267	-104.482
SVSV	II	-108.336	-110.364	-109.768	-107.305	-107.903
SVVI	II	-105.643	-108.89	-104.023	-105.851	-105.916
TVSV	II	-108.787	-110.562	-110.156	-104.234	-107.635
VDV	II	55.1194	17.8943	13.8682	42.0893	40.59307
WFDV	II	-98.5571	-99.8824	-99.2635	-94.2282	-100.216

WLAI	II	-99.5766	-99.9385	-101.655	-100.395	-99.7786
WLKV	II	-103.079	-104.941	-105.21	-98.9482	-103.83
YYKV	II	-103.498	-105.864	-105.041	-97.4754	-106.237

Table 5-4 PepCrawler scores of 27 Wild type and mutant complexes

Type	**Peptide**	**Minimum score PepCrawler reached**				
	sequence	WT	K27A	K27E	K83H	K83V
A	EAEC	-26.87	-29.96	-24.82	-31.24	-27.47
A	RNQK	-19.91	-17.9	-14.5	-21.38	-22.42
I	ETCI	-51.4	-54.01	-45.89	-54.6	-66.93
I	ETVA	-36.4	-34.97	-32.43	-43.49	-37.14
I	GSIV	-62.48	-59.04	-53.09	-57.14	-56.37
I	QSAV	-45.37	-45.6	-40.3	-51.04	-57.81
I	STYV	-55.77	-52.92	-48.03	-62.41	-53.19
I	TTRV	-53.26	-56.39	-51.01	-54.01	-56.14
II	AMPV	NA	NA	NA	NA	NA
II	DVPV	NA	NA	NA	NA	NA
II	EIAC	-34.92	-34.28	-34.8	-41.6	-42.78
II	EWYV	-57.81	-53.06	-56.3	-61.67	-61.72
II	IPEV	NA	NA	NA	NA	NA
II	LNAV	-52.79	-59.4	-53.22	-58.1	-56.35
II	NLVI	-57.8	-67.33	-70.24	-78.58	-78.77
II	SFLV	-65	-59.68	-55.02	-63.25	-66.59
II	SVEV	-66.21	-55.57	-54.52	-57.96	-69.67
II	SVIM	-51.51	-47.47	-44.68	-48.64	-53.39
II	SVKI	-61.89	-57.1	-49.55	-70.62	-67.17
II	SVSV	-58.36	-51.56	-60.09	-61.06	-65.09
II	SVVI	-63.91	-69.27	-62.93	-79.05	-68.6
II	TVSV	-55.85	-55.09	-59.12	-64.86	-68.94
II	VDV	-53.35	-54.11	-49.24	-62.07	-64.53
II	WFDV	-50.98	-61.47	-50.51	-59.63	-62.52
II	WLAI	-72.28	-72.65	-56.84	-60.99	-70.71
II	WLKV	-57.37	-59.62	-61.95	-68.17	-70.43
II	YYKV	-60.58	-59.27	-62.3	-72.38	-63.06

Table 5-5 X-Score output of the set of 27 PICK1-peptide complexes

Type	Peptide	X-Score Predicted Binding energies(kcal/mol)				
	sequence	WT	K27A	K27E	K83H	K83V
A	EAEC	-6.88	-6.867	-6.8884	-6.8187	-6.83
A	RNQK	-6.7621	-6.7669	-6.7499	-6.7543	-6.7305
I	ETCI	-7.4793	-7.4799	-7.5181	-7.4434	-7.4976
I	ETVA	-7.4931	-7.4726	-7.4868	-7.4318	-7.4717
I	GSIV	-7.3207	-7.2962	-7.3445	-7.2404	-7.2695
I	QSAV	-7.1522	-7.1399	-7.1666	-7.1023	-7.1051
I	STYV	-8.0123	-7.9865	-8.006	-8.0043	-7.9794
I	TTRV	-7.4935	-7.4636	-7.4563	-7.4525	-7.409
II	AMPV	-7.6892	-7.6633	-7.683	-7.6519	-7.5935
II	DVPV	-7.7417	-7.7303	-7.7491	-7.682	-7.6904
II	EIAC	-7.3398	-7.3338	-7.3309	-7.2516	-7.2747
II	EWYV	-8.6431	-8.6438	-8.6356	-8.5669	-8.5794
II	IPEV	-7.692	-7.6687	-7.6859	-7.637	-7.4131
II	LNAV	-7.6504	-7.6432	-7.6472	-7.6054	-7.575
II	NLVI	-8.0234	-8.0071	-8.0202	-7.9723	-7.9893
II	SFLV	-8.2788	-8.2618	-8.2633	-8.1842	-8.1645
II	SVEV	-7.475	-7.4455	-7.4891	-7.4233	-7.4488
II	SVIM	-7.4309	-7.4529	-7.4174	-7.3692	-7.388
II	SVKI	-7.5891	-7.5902	-7.5925	-7.5519	-7.5356
II	SVSV	-7.5778	-7.5514	-7.5847	-7.5735	-7.4898
II	SVVI	-7.9898	-7.9611	-7.9937	-7.8957	-7.9227
II	TVSV	-7.7828	-7.7737	-7.7909	-7.7614	-7.6985
II	VDV2	-6.603	-6.5244	-6.4845	-6.5733	-6.4345
II	WFDV	-8.5538	-8.5591	-8.5536	-8.4942	-8.4282
II	WLAI	-8.3589	-8.3467	-8.3219	-8.3281	-8.3632
II	WLKV	-8.1746	-8.1701	-8.1908	-8.1201	-8.1328
II	YYKV	-8.293	-8.287	-8.3055	-8.2151	-8.1635

Table 5-6 Experimental data from Madsen et al [33]used for comparison with the FlexPepDock, PepCrawler and X-Score results

Binding Affinities (Madsen et al 2005)			
	WT	K83V	K83H
WLKV	2,3	1,02	21
WLKI	9,5	ND	24
WLKL	37	ND	64
WLKA	49	ND	90
WLKD	>1000	>1000	>1000
WSKV	42	ND	1,1
QLAV	1,70	ND	10,4
QSAV	33	5,5	0,54
QSAI	77	ND	1,46
QSAL	166	ND	4,6
QSAA	40	ND	0,34
DSLL	245	230	210
DSLV	63	170	31

*Experimental data comprises of the K_i values from Fluorescence Polarization experiments in μM, higher values implying lower affinity (ND: Not Determined)

Table 5-7 FlexPepDock scores under different scoring functions and anchor residues

		Peptide anchor: P(-2)			**Peptide anchor: P(0)**		
Type	Peptide Sequence	Standard scoring function	Only attractive, hbond and solvation terms included	Repulsive term discarded	Standard scoring function	Only attractive, hbond and solvation terms included	Repulsive term discarded
I	DSLV	-113.78	-204.179	-171.06	-111.022	-262.292	-171.578
I	ETCI	-100.918	-202.713	-169.299	-97.576	-247.404	-165.119
I	ETMA	4677.695	-207.508	-171.212	-106.033	-245.106	-172.045
I	ETVA	-113.189	-202.464	-170.746	-109.243	-246.85	-168.566
I	GSIV	-111.124	-202.715	-169.036	-110.605	-252.467	-170.06
I	GSKA	6676.661	-202.889	-163.38	2516.497	-244.701	-167.506
I	NTVV	1795.854	-206.594	-173.041	14732.61	-251.627	-172.481
I	QSAA	-110.281	-200.165	-163.444	-106.463	-220.979	-163.574
I	QSAI	-108.342	-203.528	-165.786	-108.137	-258.578	-167.03

I	QSAL	-108.741	-204.333	-167.88	-108.504	-260.776	-165.87
I	QSAV	-106.391	-199.834	-162.05	-110.815	-253.302	-163.22
I	STYV	-109.232	-204.488	-176.091	-108.975	-268.575	-177.23
I	TSSL	11076.41	-206.898	-170.265	10196.71	-265.824	-170.084
I	TTRV	-110.678	-206.828	-173.625	-111.661	-248.977	-170.806
I	WSKV	-105.915	-208.01	-178.49	-104.455	-260.688	-177.574
II	AMPV	-111.926	-203.505	-175.564	-111.859	-269.244	-172.029
II	DVPV	-100.405	-203.449	-175.992	-111.825	-240.615	-172.835
II	EIAC	-105.96	-201.573	-171.311	-105.299	-237.467	-169.505
II	EWYV	-108.865	-207.676	-188.398	-108.951	-278.544	-186.659
II	GIQV	6540.258	-206.606	-171.846	-78.887	-218.285	-173.165
II	IPEV	-101.521	-207.084	-179.413	-105.645	-269.953	-176.664
II	LNAV	-103.633	-200.963	-167.635	-105.041	-239.189	-167.354
II	NLVI	-103.125	-206.745	-177.716	-107.526	-267.065	-175.666
II	PMPV	4893.257	-207.876	-177.701	120.742	-270.434	-179.011
II	QLAV	-108.939	-204.713	-173.616	-103.854	-254.023	-171.632
II	SFVL	-104.802	-206.227	-178.295	-105.271	-247.012	-176.817
II	SIKI	4158.164	-210.395	-176.577	7884.46	-249.29	-177.386
II	SVEV	-111.65	-204.022	-171.104	-111.363	-247.139	-170.191
II	SVIM	-109.979	-207.107	-177.524	-111.538	-266.62	-173.45
II	SVKI	-108.401	-205.11	-173.017	-108.017	-242.354	-171.602
II	SVSV	-109.464	-202.241	-169.952	-110.739	-231.628	-170.245
II	SVVI	-110.236	-205.213	-175.601	-110.687	-264.058	-173.208
II	TVSV	-96.261	-203.756	-172.785	-111.084	-257.227	-170.809
II	VDV	-106.985	-200.611	-169.155			
II	WFDV	-105.375	-210.089	-190.692	-108.037	-270.872	-190.536
II	WLAI	-108.948	-210.386	-187.55	-106.462	-261.519	-186.109
II	WLKA	-112.589	-208.871	-182.858	-106.803	-244.215	-183.223
II	WLKI	484.96	-219.442	-198.364	-86.45	-288.373	-194.633
II	WLKL	2090.986	-216.546	-190.593	275.87	-267.186	-172.565
II	WLKV	-104.7	-217.876	-199.464	715.441	-223.808	-192.807
II	YYKV	-106.697	-213.482	-197.577	-50.76	-289.351	-191.431
A	RNQK	65.514	-203.379	-170.229	1000.249	-264.23	-165.637
A	DFTC	-85.759	-207.86	-176.186	-84.781	-261.308	-176.334
A	MKPK	6627.794	-210.213	-177.552	1397.545	-274.152	-180.851
A	EAEC	-105.485	-200.841	-165.011	-104.817	-258.201	-162.968
A	PPTV	9794.667	-204.813	-172.448	11759.78	-267.318	-173.086

A	ETCG	-110.722	-198.415	-160.774	-68.528	-243.437	-161.802
A	ETMR	1879.037	-207.478	-175.97	518.269	-254.54	-171.02
A	ETVC	-108.668	-200.955	-168.67	-109.218	-247.711	-164.512
A	GSIK	-104.712	-202.231	-167.528	-0.656	-258.41	-166.744
A	GSKH	-103.205	-202.323	-165.066	-103.109	-250.106	-165.624
A	KKNK	4297.371	-208.081	-174.359	2623.488	-268.338	-178.038
A	NTVK	1.229	-203.576	-168.515	-102.594	-234.661	-168.178
A	QSAK	484.386	-201.431	-161.212	-103.555	-225.509	-162.298
A	STYC	-106.098	-199.478	-172.283	-106.231	-228.077	-167.842
A	TSSD	-108.632	-201.188	-164.584	-108.725	-256.547	-164.165
A	TTRE	-93.046	-206.108	-171.628	-107.268	-255.912	-169.094
III	EECI	3019.67	-207.465	-173.939	782.182	-259.124	-174.739
III	EEMA	2848.202	-208.136	-173.081	-106.3	-268.589	-173.791
III	EEVA	5574.443	-205.69	-171.38	-103.831	-264.335	-169.258
III	GDIV	8766.177	-207.743	-173.374	12086.6	-261.492	-175.169
III	GDKA	5860.405	-203.414	-163.593	2576.878	-255.571	-163.676
III	NEVV	3840.28	-208.44	-174.153	4839.346	-258.416	-172.523
III	QDAV	8347.519	-205.458	-171.969	-103.291	-262.15	-168.42
III	SEYV	2028.845	-213.249	-180.402	5778.768	-252.483	-180.819
III	TDSL	12872.35	-207.753	-170.89	4864.928	-244.123	-172.766
III	TERV	7274.809	-207.808	-175.214	5554.682	-218.636	-174.068
N	DSLL	-111.145	-207.164	-174.477	-107.899	-262.779	-173.002
N	WLKD	-105.934	-208.656	-183.941	-105.208	-275.145	-183.503

Table 5-8 Scores from Standard runs of FlexPepDock, PepCrawler and X-Score listed from most favorable energy complexes to the least for each one

FlexPepDock		PepCrawler		X-Score	
K27A_ETVA	-114.84	WLKL_K83V	-81.52	K27A_EWYV	-8.6438
K27E_ETVA	-114.529	K83H_SVVI	-79.05	EWYV	-8.6431
K27E_AMPV	-113.41	K83V_NLVI	-78.77	K27E_EWYV	-8.6356
QSAA_K27A	-112.375	K83H_NLVI	-78.58	K83V_EWYV	-8.5794
ETVA	-112.227	WLKV_K83V	-73.97	K83H_EWYV	-8.5669
K83H_ETVA	-112.048	K27A_WLAI	-72.65	K27A_WFDV	-8.5591
QSAA_K27E	-111.921	K83H_YYKV	-72.38	WFDV	-8.5538
K83V_ETVA	-111.648	WLKI_K83V	-72.29	K27E_WFDV	-8.5536
AMPV	-111.392	WLAI	-72.28	K83H_WFDV	-8.4942
K27E_LNAV	-111.347	K83V_WLAI	-70.71	K83V_WFDV	-8.4282
K27A_DVPV	-111.006	K83H_SVKI	-70.62	WLKL	-8.3818
QLAV_K27A	-110.784	K83V_WLKV	-70.43	WLKI	-8.3663
K27A_TVSV	-110.562	WLKI_K83H	-70.28	K83V_WLAI	-8.3632
K27E_QSAV	-110.479	K27E_NLVI	-70.24	WLAI	-8.3589
K27A_SVSV	-110.364	DSLL_K27A	-70.23	K27A_WLAI	-8.3467
K83V_AMPV	-110.337	WLKI	-69.8	WLKL_K83V_	-8.3301
QSAA	-110.316	K83V_SVEV	-69.67	WLKI_K27A_	-8.3295
QSAA_K83V	-110.293	K27A_SVVI	-69.27	K83H_WLAI	-8.3281
QSAV_K27E	-110.282	K83V_TVSV	-68.94	K27E_WLAI	-8.3219
K27E_DVPV	-110.249	K83V_SVVI	-68.6	WLKI_K83V_	-8.3161
K27A_GSIV	-110.205	K83H_WLKV	-68.17	WLKI_K83H_	-8.3132
K27E_TVSV	-110.156	K27A_NLVI	-67.33	K27E_YYKV	-8.3055
K27E_GSIV	-110.066	K83V_SVKI	-67.17	WLKL_K27A_	-8.303
QSAV_K27A	-110.045	K83V_ETCI	-66.93	WLKL_K27E_	-8.2944
K27A_NLVI	-109.984	K83V_SFLV	-66.59	WLKI_K27E_	-8.2937
K83H_AMPV	-109.965	SVEV	-66.21	YYKV	-8.293
K27E_STYV	-109.892	QLAV_K83V	-65.95	K27A_YYKV	-8.287
DSLV_K27A	-109.869	WLKL	-65.38	WLKL_K83H_	-8.2812
K27E_SVSV	-109.768	K83V_SVSV	-65.09	SFLV	-8.2788
K27A_EIAC	-109.748	SFLV	-65	K27E_SFLV	-8.2633
QSAV	-109.581	K83H_TVSV	-64.86	K27A_SFLV	-8.2618
QLAV_K27E	-109.439	K83V_VDV	-64.53	WLKV_K27E_	-8.2521
DSLV_K27E	-109.281	DSLV_K83H	-63.98	WLKV_K83V_	-8.2345
ETVC	-109.238	SVVI	-63.91	WLKV_K83H_	-8.2326

K27A_EAEC	-109.162	K83H_SFLV	-63.25	K83H_YYKV	-8.2151
K83H_LNAV	-109.156	K83V_YYKV	-63.06	K27E_WLKV	-8.1908
QLAV_K83V	-109.135	WLKL_K83H	-62.97	K83H_SFLV	-8.1842
K27A_STYV	-109.093	K27E_SVVI	-62.93	WLKV	-8.1746
K27E_EAEC	-109.052	K83V_WFDV	-62.52	K27A_WLKV	-8.1701
K27A_AMPV	-109.035	GSIV	-62.48	K83V_SFLV	-8.1645
K27E_TTRV	-108.938	K83H_STYV	-62.41	K83V_YYKV	-8.1635
K27A_SVVI	-108.89	K27E_YYKV	-62.3	WLKV_K27A_	-8.1499
TVSV	-108.787	K83H_VDV	-62.07	K83V_WLKV	-8.1328
K27A_EWYV	-108.662	K27E_WLKV	-61.95	K83H_WLKV	-8.1201
K27A_TTRV	-108.526	SVKI	-61.89	WLKA_K27A_	-8.0408
K27E_EWYV	-108.487	WLKV_K83H	-61.82	NLVI	-8.0234
K27A_SVEV	-108.373	K83V_EWYV	-61.72	K27E_NLVI	-8.0202
STYC	-108.352	K83H_EWYV	-61.67	STYV	-8.0123
SVSV	-108.336	K27A_WFDV	-61.47	K27A_NLVI	-8.0071
ETCG	-108.263	K83H_SVSV	-61.06	K27E_STYV	-8.006
K83V_DVPV	-108.215	K83H_WLAI	-60.99	K83H_STYV	-8.0043
TSSD	-108.171	YYKV	-60.58	K27E_SVVI	-7.9937
DVPV	-108.094	WLKI_K27E	-60.56	SVVI	-7.9898
QLAV	-108.045	DSLV_K83V	-60.46	K83V_NLVI	-7.9893
K27A_LNAV	-107.932	K27E_SVSV	-60.09	WLKA_K83H_	-7.9872
K83V_SVSV	-107.903	QLAV_K83H	-60.04	K27A_STYV	-7.9865
DSLV	-107.869	K27A_SFLV	-59.68	K83V_STYV	-7.9794
QSAA_K83H	-107.865	K83H_WFDV	-59.63	K83H_NLVI	-7.9723
K83V_TTRV	-107.805	K27A_WLKV	-59.62	K27A_SVVI	-7.9611
K83V_QSAV	-107.723	K27A_LNAV	-59.4	WLKA_K27E_	-7.9376
K83V_LNAV	-107.718	K27A_YYKV	-59.27	K83V_SVVI	-7.9227
STYV	-107.689	WLKV_K27A	-59.2	WLKA	-7.922
GSIV	-107.644	SIKI	-59.13	WLKD	-7.8988
K83V_TVSV	-107.635	K27E_TVSV	-59.12	K83H_SVVI	-7.8957
EAEC	-107.629	K27A_GSIV	-59.04	WLKD_K83V_	-7.8951
K27E_NLVI	-107.62	SVSV	-58.36	WLKA_K83V_	-7.8902
K27E_EIAC	-107.609	K83H_LNAV	-58.1	WLKD_K27E_	-7.8853
K83V_GSIV	-107.567	K83H_SVEV	-57.96	WLKD_K83H_	-7.8827
QSAI_K27A	-107.455	EWYV	-57.81	WLKD_K27A_	-7.8719
QSAI_K27E	-107.429	K83V_QSAV	-57.81	WSKV_K27E_	-7.8097
K83H_SVSV	-107.305	NLVI	-57.8	WSKV_K27A_	-7.7962

K83H_DVPV	-107.28	NTVV	-57.54	K27E_TVSV	-7.7909
K83V_STYV	-107.102	WLKV	-57.37	TVSV	-7.7828
QSAV_K83V	-107.061	K83H_GSIV	-57.14	K27A_TVSV	-7.7737
EIAC	-107.028	K27A_SVKI	-57.1	K83H_TVSV	-7.7614
K83V_NLVI	-106.977	WLKV_K27E	-56.95	K27E_DVPV	-7.7491
K83V_EIAC	-106.947	K27E_WLAI	-56.84	DVPV	-7.7417
DSLV_K83V	-106.738	DSLL_K83V	-56.51	K27A_DVPV	-7.7303
QLAV_K83H	-106.581	K27A_TTRV	-56.39	WSKV_K83H_	-7.7093
K27E_SVIM	-106.503	K83V_GSIV	-56.37	WSKV	-7.6989
NLVI	-106.466	QSAV_K83V	-56.37	K83V_TVSV	-7.6985
K27A_IPEV	-106.459	K83V_LNAV	-56.35	IPEV	-7.692
K83H_NLVI	-106.452	K27E_EWYV	-56.3	K83V_DVPV	-7.6904
K27E_SFLV	-106.406	QSAL_K27E	-56.24	AMPV	-7.6892
TTRV	-106.294	K83V_TTRV	-56.14	K27E_IPEV	-7.6859
K83H_STYV	-106.282	QSAI_K27E	-56.08	K27E_AMPV	-7.683
WLKA_K27A	-106.252	TVSV	-55.85	K83H_DVPV	-7.682
LNAV	-106.209	STYV	-55.77	QLAV	-7.6723
K83H_EIAC	-106.155	QLAV_K27A	-55.73	WSKV_K83V_	-7.6692
K83H_GSIV	-106.077	K27A_SVEV	-55.57	K27A_IPEV	-7.6687
K27E_SVKI	-106.05	K27A_TVSV	-55.09	STYC	-7.6645
K83V_EAEC	-106.046	GDIV	-55.02	K27A_AMPV	-7.6633
EWYV	-105.993	K27E_SFLV	-55.02	QLAV_K27E_	-7.6619
K83H_SVEV	-105.971	QSAI_K83V	-55.02	QLAV_K27A_	-7.6586
K83V_SVVI	-105.916	QLAV	-54.95	K83H_AMPV	-7.6519
K83V_EWYV	-105.913	K83H_ETCI	-54.6	LNAV	-7.6504
K27E_IPEV	-105.909	K27E_SVEV	-54.52	K27E_LNAV	-7.6472
K27A_YYKV	-105.864	WSKV_K83V	-54.46	K27A_LNAV	-7.6432
K83H_SVVI	-105.851	QSAL_K83V	-54.39	K83H_IPEV	-7.637
SVEV	-105.849	QSAL	-54.22	QLAV_K83H_	-7.6138
K83V_SVEV	-105.764	K27A_VDV	-54.11	QLAV_K83V_	-7.6117
SVVI	-105.643	WLKL_K27E	-54.06	K83H_LNAV	-7.6054
K27A_SFLV	-105.627	K27A_ETCI	-54.01	K83V_AMPV	-7.5935
WLKA_K27E	-105.624	K83H_TTRV	-54.01	K27E_SVKI	-7.5925
QSAV_K83H	-105.618	WLKL_K27A	-53.9	K27A_SVKI	-7.5902
WLKV_K27E	-105.603	WSKV	-53.87	SVKI	-7.5891
K27E_ETCI	-105.517	QLAV_K27E	-53.71	K27E_SVSV	-7.5847
K27A_SVKI	-105.472	K83V_SVIM	-53.39	DSLL_K27E_	-7.58

QSAL_K27A	-105.434	VDV	-53.35	SVSV	-7.5778
QSAK	-105.394	TTRV	-53.26	K83V_LNAV	-7.575
K83H_QSAV	-105.274	K27E_LNAV	-53.22	K83H_SVSV	-7.5735
K27E_WLKV	-105.21	K83V_STYV	-53.19	DSLL	-7.5594
QSAI_K83V	-105.105	K27E_GSIV	-53.09	K83H_SVKI	-7.5519
GSIK	-105.055	K27A_EWYV	-53.06	K27A_SVSV	-7.5514
K27E_YYKV	-105.041	K27A_STYV	-52.92	SEYV	-7.5493
QSAL_K27E	-104.967	LNAV	-52.79	K83V_SVKI	-7.5356
NTVK	-104.958	QSAI_K83H	-52.62	K27E_ETCI	-7.5181
K27A_WLKV	-104.941	QSAV_K83H	-52.56	DSLL_K27A_	-7.5078
K83H_EAEC	-104.784	DSLV	-52.32	K83V_ETCI	-7.4976
ETMR	-104.549	DSLV_K27A	-51.79	TTRV	-7.4935
K27E_SVEV	-104.496	TDSL	-51.7	ETVA	-7.4931
K83V_SVKI	-104.482	K27A_SVSV	-51.56	K83V_SVSV	-7.4898
QSAI	-104.471	SVIM	-51.51	K27E_SVEV	-7.4891
K83V_SVIM	-104.414	WLKI_K27A	-51.49	K27E_ETVA	-7.4868
K83H_TVSV	-104.234	DSLL	-51.43	K27A_ETCI	-7.4799
TTRE	-104.208	WSKV_K27A	-51.43	ETCI	-7.4793
K27E_RNQK	-104.143	ETCI	-51.4	DSLL_K83V_	-7.475
DSLV_K83H	-104.035	K83H_QSAV	-51.04	SVEV	-7.475
WLKA_K83H	-104.032	K27E_TTRV	-51.01	GDIV	-7.4743
K27E_SVVI	-104.023	WFDV	-50.98	DSLV_K27E_	-7.4731
K27A_RNQK	-104.018	DSLV_K27E	-50.94	K27A_ETVA	-7.4726
IPEV	-103.964	QSAL_K83H	-50.88	K83V_ETVA	-7.4717
WLKV_K83V	-103.896	NEVV	-50.72	DSLV	-7.4702
K83H_TTRV	-103.868	K27E_WFDV	-50.51	K27A_TTRV	-7.4636
K83V_WLKV	-103.83	QSAI	-50.2	K27E_TTRV	-7.4563
WSKV_K83H	-103.621	WSKV_K83H	-50.11	K27A_SVIM	-7.4529
K27A_QSAV	-103.517	K27E_SVKI	-49.55	K83H_TTRV	-7.4525
YYKV	-103.498	QSAL_K27A	-49.25	K83V_SVEV	-7.4488
WSKV_K83V	-103.438	K27E_VDV	-49.24	DSLV_K27A_	-7.4476
K83V_SFLV	-103.358	SEYV	-49.24	DSLL_K83H_	-7.4463
RNQK	-103.296	K83H_SVIM	-48.64	K27A_SVEV	-7.4455
WLKA_K83V	-103.267	K27E_STYV	-48.03	K83H_ETCI	-7.4434
K83H_SVKI	-103.267	K27A_SVIM	-47.47	K83H_ETVA	-7.4318
QSAI_K83H	-103.164	WLKA_K83V	-46.13	SVIM	-7.4309
WLKV	-103.079	EECI	-45.9	K83H_SVEV	-7.4233

K83V_ETCI	-103.02	K27E_ETCI	-45.89	K27E_SVIM	-7.4174
K27A_SVIM	-102.924	DSLL_K83H	-45.71	K83V_IPEV	-7.4131
QSAL_K83H	-102.768	K27A_QSAV	-45.6	K83V_TTRV	-7.409
QSAL	-102.672	QSAV	-45.37	NTVK	-7.4039
WLKI_K27A	-102.655	K27E_SVIM	-44.68	ETVC	-7.3959
DSLL_K27E	-102.652	QSAV_K27E	-44.68	K83V_SVIM	-7.388
K83H_ETCI	-102.644	QSAV_K27A	-44.59	K83H_SVIM	-7.3692
K83H_IPEV	-102.638	DSLL_K27E	-44.27	DSLV_K83H_	-7.3529
WLKV_K27A	-102.615	EEVA	-43.96	DSLV_K83V_	-7.3496
WLKA	-102.473	DFTC	-43.68	K27E_GSIV	-7.3445
QSAL_K83V	-102.443	K83H_ETVA	-43.49	NTVV	-7.3407
K83H_RNQK	-102.337	WLKA	-43.07	EIAC	-7.3398
SVIM	-102.316	K83V_EIAC	-42.78	QSAI_K27E_	-7.3389
K83H_SVIM	-102.208	TSSL	-42.08	QSAL_K27A_	-7.3368
SVKI	-101.986	K83H_EIAC	-41.6	K27A_EIAC	-7.3338
K27A_ETCI	-101.96	QSAI_K27A	-41.48	QSAL	-7.332
WSKV_K27E	-101.857	WSKV_K27E	-41.1	K27E_EIAC	-7.3309
WLKV_K83H	-101.854	K27E_QSAV	-40.3	QSAI	-7.3289
WSKV_K27A	-101.853	WLKA_K83H	-39.13	GSIV	-7.3207
K27E_WLAI	-101.655	TERV	-38.06	QSAL_K27E_	-7.3207
K83V_RNQK	-101.394	ETVC	-37.55	QSAI_K27A_	-7.3144
WLKI	-101.351	WLKD_K83V	-37.25	K27A_GSIV	-7.2962
WLKI_K83V	-100.787	K83V_ETVA	-37.14	K83V_EIAC	-7.2747
DSLL_K83V	-100.422	ETVA	-36.4	K83V_GSIV	-7.2695
K83H_WLAI	-100.395	WLKD_K83H	-35.87	QSAL_K83V_	-7.2597
K83H_SFLV	-100.271	STYC	-35.02	K83H_EIAC	-7.2516
K83V_WFDV	-100.216	K27A_ETVA	-34.97	TTRE	-7.2472
WLKD_K27A	-100.079	EIAC	-34.92	K83H_GSIV	-7.2404
SFLV	-99.9782	GSKH	-34.91	QSAI_K83V_	-7.2242
K27A_WLAI	-99.9385	K27E_EIAC	-34.8	QSAL_K83H_	-7.22
K27A_WFDV	-99.8824	GIQV	-34.34	QSAV_K27E_	-7.2015
K83H_EWYV	-99.871	K27A_EIAC	-34.28	QSAI_K83H_	-7.1986
K83V_WLAI	-99.7786	K27E_ETVA	-32.43	QSAV_K27A_	-7.1895
DSLL_K27A	-99.7514	WLKA_K27A	-31.94	K27E_QSAV	-7.1666
WLKD_K27E	-99.5969	WLKD	-31.45	QSAV	-7.1522
WLAI	-99.5766	K83H_EAEC	-31.24	SIKI	-7.1509
WLKI_K83H	-99.5702	WLKD_K27A	-30.99	PPTV	-7.1479

ETCI	-99.5578	GSIK	-30.54	K27A_QSAV	-7.1399
WLKL_K83V	-99.3959	QDAV	-30.22	QSAV_K83V_	-7.1345
K27E_WFDV	-99.2635	K27A_EAEC	-29.96	NEVV	-7.1308
WLKI_K27E	-99.1398	WLKA_K27E	-29.49	QSAV_K83H_	-7.1182
WLKD_K83V	-99.0832	NTVK	-28.72	K83V_QSAV	-7.1051
K83H_WLKV	-98.9482	WLKD_K27E	-28.43	K83H_QSAV	-7.1023
WFDV	-98.5571	QSAA_K83V	-28.07	DFTC	-7.0708
DSLL	-98.4145	ETMR	-27.94	GIQV	-7.066
WLKD	-98.369	K83V_EAEC	-27.47	TSSD	-7.0373
DSLL_K83H	-98.1481	EAEC	-26.87	GSIK	-7.0321
K83H_YYKV	-97.4754	EEMA	-26.68	K27E_EAEC	-6.8884
WLKL_K27A	-97.0138	TTRE	-26.44	ETMR	-6.8848
GSKH	-95.1494	ETCG	-25.54	QSAA	-6.8844
WLKL	-94.896	QSAA_K83H	-24.97	QSAK	-6.8819
WLKL_K27E	-94.6335	K27E_EAEC	-24.82	EAEC	-6.88
K83H_WFDV	-94.2282	ETMA	-23.65	PMPV	-6.8792
WSKV	-94.1114	QSAA	-23.16	K27A_EAEC	-6.867
K83V_IPEV	-94.1	QSAA_K27A	-23.14	QSAA_K27E_	-6.8637
WLKL_K83H	-92.8201	QSAA_K27E	-22.6	TERV	-6.8634
WLKD_K83H	-76.8556	K83V_RNQK	-22.42	QSAA_K27A_	-6.857
GSKA	-73.2198	K83H_RNQK	-21.38	GSKH	-6.8457
KKNK	-61.2344	RNQK	-19.91	K83V_EAEC	-6.83
SEYV	-60.5019	K27A_RNQK	-17.9	K83H_EAEC	-6.8187
GIQV	-55.1745	KKNK	-17.82	ETCG	-6.8062
GDKA	-55.0677	QSAK	-16.99	QSAA_K83V_	-6.7985
PMPV	-52.4265	TSSD	-16.65	EEVA	-6.7878
EEMA	-51.7932	K27E_RNQK	-14.5	QSAA_K83H_	-6.7766
MKPK	-50.0327	GDKA	-13.96	K27A_RNQK	-6.7669
PPTV	-49.8485	GSKA	-13.2	RNQK	-6.7621
QDAV	-46.9867	AMPV	NA	K83H_RNQK	-6.7543
ETMA	-44.6773	DVPV	NA	K27E_RNQK	-6.7499
EEVA	-33.8158	IPEV	NA	K83V_RNQK	-6.7305
TDSL	-28.5521	K27A_AMPV	NA	TDSL	-6.6885
TSSL	-27.3073	K27A_DVPV	NA	QDAV	-6.6759
GDIV	-24.5791	K27A_IPEV	NA	EECI	-6.6688
EECI	-18.8814	K27E_AMPV	NA	TSSL	-6.6269
SIKI	-18.0724	K27E_DVPV	NA	VDV	-6.603

NTVV	-17.5168	K27E_IPEV	NA	K83H_VDV	-6.5733
TERV	-13.8444	K83H_AMPV	NA	MKPK	-6.5724
NEVV	-11.1379	K83H_DVPV	NA	K27A_VDV	-6.5244
K83V_VDV	0	K83H_IPEV	NA	ETMA	-6.4861
K83V_YYKV	0	K83V_AMPV	NA	K27E_VDV	-6.4845
DFTC	13.5544	K83V_DVPV	NA	K83V_VDV	-6.4345
K27E_VDV	13.8682	K83V_IPEV	NA	GDKA	-6.4182
K27A_VDV	17.8943	MKPK	NA	KKNK	-6.3958
K83H_VDV	42.0893	PMPV	NA	EEMA	-6.2871
VDV	55.1194	PPTV	NA	GSKA	-6.1682

Table 5-9 FlexPepDock scores of complexes used in Madsen et al. under different scoring schemes and with different anchor residues

	Peptide anchor: P(-2)	**Peptide anchor: P(0)**	**Only attractive, hbond and solvation terms included**	**Repulsive term discarded**
WLKD	-65.841	-69.784	-275.004	-183.941
WLKL	1804.061	-64.39	-272.25	-198.364
WLKI	-40.151	-37.559	-287.193	-190.593
WLKA	-72.998	-68.818	-278.789	-182.858
WLKV	-65.946	795.091	-288.976	-199.464
WSKV	-67.593	-64.313	-279.528	-178.49
QLAV	-70.483	-65.464	-246.123	-173.616
QSAV	-68.188	-71.252	-233.497	-162.05
QSAI	-69.837	-70.035	-257.876	-165.786
QSAL	-70.949	-70.738	-259.22	-167.88
QSAA	-70.156	-67.52	-222.931	-163.444
DSLL	-71.366	-69.351	-247.69	-174.477
DSLV	-71.705	-71.369	-237.807	-171.06
WLKD_K83H	190.014	639.781	-280.841	-194.622
WLKI_K83H	-63.974	25.989	-285.742	-200.225
WLKL_K83H	-70.428	-69.662	-275.375	-189.929
WLKA_K83H	-58.226	613.839	-286.567	-193.735
WLKV_K83H	-40.906	-67.133	-291.167	-192.167
WSKV_K83H	570.95	308.408	-221.88	-191.367
QLAV_K83H	35.871	-68.685	-262.216	-173.589
QSAV_K83H	-65.443	-70.238	-246.431	-167.496

QSAI_K83H	-66.321	-66.303	-259.124	-168.935
QSAL_K83H	-67.534	-67.098	-228.726	-165.092
QSAA_K83H	-67.986	-64.87	-253.66	-164.581
DSLL_K83H	-70.862	-68.565	-228.136	-172.569
DSLV_K83H	-69.931	-70.349	-265.341	-172.304
WLKV_K83V	18.528	-64.475	-223.634	-194.677
WLKD_K83V	-69.489	-67.521	-268.814	-183.911
QSAV_K83V	-66.739	-71.157	-259.29	-163.783
DSLL_K83V	-69.934	-70.648	-264.596	-172.731
DSLV_K83V	-71.614	-71.407	-258.77	-170.599

BIBLIOGRAPHY

BIBLIOGRAPHY

1. Xu, J. and J. Xia, *Structure and function of PICK1.* Neurosignals, 2006. **15**(4): p. 190-201.
2. Xia, J., et al., *Clustering of AMPA receptors by the synaptic PDZ domain-containing protein PICK1.* Neuron, 1999. **22**(1): p. 179-87.
3. Ranganathan, R. and E.M. Ross, *PDZ domain proteins: scaffolds for signaling complexes.* Curr Biol, 1997. **7**(12): p. R770-3.
4. Raveh, B., et al., *Rosetta FlexPepDock ab-initio: simultaneous folding, docking and refinement of peptides onto their receptors.* PLoS One, 2011. **6**(4): p. e18934.
5. Donsky, E. and H.J. Wolfson, *PepCrawler: a fast RRT-based algorithm for high-resolution refinement and binding affinity estimation of peptide inhibitors.* Bioinformatics, 2011. **27**(20): p. 2836-42.
6. Wang, R., Y. Lu, and S. Wang, *Comparative evaluation of 11 scoring functions for molecular docking.* J Med Chem, 2003. **46**(12): p. 2287-303.
7. Staudinger, J., et al., *PICK1: a perinuclear binding protein and substrate for protein kinase C isolated by the yeast two-hybrid system.* J Cell Biol, 1995. **128**(3): p. 263-71.
8. Peter, B.J., et al., *BAR domains as sensors of membrane curvature: the amphiphysin BAR structure.* Science, 2004. **303**(5657): p. 495-9.
9. Jin, W., et al., *Lipid binding regulates synaptic targeting of PICK1, AMPA receptor trafficking, and synaptic plasticity.* J Neurosci, 2006. **26**(9): p. 2380-90.
10. Citri, A., et al., *Calcium binding to PICK1 is essential for the intracellular retention of AMPA receptors underlying long-term depression.* J Neurosci, 2010. **30**(49): p. 16437-52.
11. Boudin, H. and A.M. Craig, *Molecular determinants for PICK1 synaptic aggregation and mGluR7a receptor coclustering: role of the PDZ, coiled-coil, and acidic domains.* J Biol Chem, 2001. **276**(32): p. 30270-6.
12. Focant, M.C., et al., *PICK1 expression in reactive astrocytes within the spinal cord of ALS rats.* Neuropathol Appl Neurobiol, 2012.
13. Dev, K.K. and J.M. Henley, *The schizophrenic faces of PICK1.* Trends Pharmacol Sci, 2006. **27**(11): p. 574-9.
14. Atianjoh, F.E., et al., *Spinal cord protein interacting with C kinase 1 is required for the maintenance of complete Freund's adjuvant-induced inflammatory pain but not for incision-induced post-operative pain.* Pain, 2010. **151**(1): p. 226-34.
15. Bell, J.D., et al., *PICK1-mediated GluR2 endocytosis contributes to cellular injury after neuronal trauma.* Cell Death Differ, 2009. **16**(12): p. 1665-80.
16. Wang, W., et al., *Preserved acute pain and impaired neuropathic pain in mice lacking protein interacting with C Kinase 1.* Mol Pain, 2011. **7**: p. 11.
17. Bellone, C. and C. Luscher, *Cocaine triggered AMPA receptor redistribution is reversed in vivo by mGluR-dependent long-term depression.* Nat Neurosci, 2006. **9**(5): p. 636-41.
18. Dixon, R.M., J.R. Mellor, and J.G. Hanley, *PICK1-mediated glutamate receptor subunit 2 (GluR2) trafficking contributes to cell death in oxygen/glucose-deprived hippocampal neurons.* J Biol Chem, 2009. **284**(21): p. 14230-5.
19. Zhao, B., et al., *PICK1 promotes caveolin-dependent degradation of TGF-beta type I receptor.* Cell Res, 2012.

20. Perrin, A., et al., *Molecular cytogenetic and genetic aspects of globozoospermia: a review.* Andrologia, 2012.
21. Tonikian, R., et al., *A specificity map for the PDZ domain family.* PLoS Biol, 2008. **6**(9): p. e239.
22. Ivarsson, Y., *Plasticity of PDZ domains in ligand recognition and signaling.* FEBS Lett, 2012. **586**(17): p. 2638-47.
23. Sheng, M. and C. Sala, *PDZ domains and the organization of supramolecular complexes.* Annu Rev Neurosci, 2001. **24**: p. 1-29.
24. Harris, B.Z. and W.A. Lim, *Mechanism and role of PDZ domains in signaling complex assembly.* J Cell Sci, 2001. **114**(Pt 18): p. 3219-31.
25. Kim, E. and M. Sheng, *PDZ domain proteins of synapses.* Nat Rev Neurosci, 2004. **5**(10): p. 771-81.
26. Nakamura, Y., et al., *PICK1 inhibition of the Arp2/3 complex controls dendritic spine size and synaptic plasticity.* EMBO J, 2011. **30**(4): p. 719-30.
27. Hirbec, H., et al., *The PDZ proteins PICK1, GRIP, and syntenin bind multiple glutamate receptor subtypes. Analysis of PDZ binding motifs.* J Biol Chem, 2002. **277**(18): p. 15221-4.
28. Zhang, Y., et al., *Convergent and divergent ligand specificity among PDZ domains of the LAP and zonula occludens (ZO) families.* J Biol Chem, 2006. **281**(31): p. 22299-311.
29. Beuming, T., et al., *PDZBase: a protein-protein interaction database for PDZ-domains.* Bioinformatics, 2005. **21**(6): p. 827-8.
30. Fuh, G., et al., *Analysis of PDZ domain-ligand interactions using carboxyl-terminal phage display.* J Biol Chem, 2000. **275**(28): p. 21486-91.
31. Stiffler, M.A., et al., *PDZ domain binding selectivity is optimized across the mouse proteome.* Science, 2007. **317**(5836): p. 364-9.
32. Chen, J.R., et al., *Predicting PDZ domain-peptide interactions from primary sequences.* Nat Biotechnol, 2008. **26**(9): p. 1041-5.
33. Madsen, K.L., et al., *Molecular determinants for the complex binding specificity of the PDZ domain in PICK1.* J Biol Chem, 2005. **280**(21): p. 20539-48.
34. Thorsen, T.S., et al., *A fluorescence polarization based screening assay for identification of small molecule inhibitors of the PICK1 PDZ domain.* Comb Chem High Throughput Screen, 2011. **14**(7): p. 590-600.
35. Ammendrup-Johnsen, I., et al., *Serine 77 in the PDZ domain of PICK1 is a protein kinase Calpha phosphorylation site regulated by lipid membrane binding.* Biochemistry, 2012. **51**(2): p. 586-96.
36. Shao, X., et al., *Threonine 82 at the PDZ domain of PICK1 is critical for AMPA receptor interaction and localization.* Neurochem Int, 2010. **56**(8): p. 962-70.
37. Smith, C.A. and T. Kortemme, *Structure-based prediction of the peptide sequence space recognized by natural and synthetic PDZ domains.* J Mol Biol, 2010. **402**(2): p. 460-74.
38. Teyra, J., S.S. Sidhu, and P.M. Kim, *Elucidation of the binding preferences of peptide recognition modules: SH3 and PDZ domains.* FEBS Lett, 2012. **586**(17): p. 2631-7.
39. Hui, S. and G.D. Bader, *Proteome scanning to predict PDZ domain interactions using support vector machines.* BMC Bioinformatics, 2010. **11**: p. 507.
40. Thorsen, T.S., et al., *Identification of a small-molecule inhibitor of the PICK1 PDZ domain that inhibits hippocampal LTP and LTD.* Proc Natl Acad Sci U S A, 2010. **107**(1): p. 413-8.
41. Bach, A., et al., *Structure-activity relationships of a small-molecule inhibitor of the PDZ domain of PICK1.* Org Biomol Chem, 2010. **8**(19): p. 4281-8.

42. Bolia, A., et al., *The binding affinities of proteins interacting with the PDZ domain of PICK1.* Proteins, 2012. **80**(5): p. 1393-408.
43. Staneva, I. and S. Wallin, *Binding free energy landscape of domain-peptide interactions.* PLoS Comput Biol, 2011. **7**(8): p. e1002131.
44. Elkins, J.M., et al., *Structure of PICK1 and other PDZ domains obtained with the help of self-binding C-terminal extensions.* Protein Sci, 2007. **16**(4): p. 683-94.
45. Pan, L., et al., *Clustering and synaptic targeting of PICK1 requires direct interaction between the PDZ domain and lipid membranes.* EMBO J, 2007. **26**(21): p. 4576-87.
46. London, N., et al., *Rosetta FlexPepDock web server--high resolution modeling of peptide-protein interactions.* Nucleic Acids Res, 2011. **39**(Web Server issue): p. W249-53.
47. Feng, Y., et al., *[K83 site affects PICK1 PDZ binding ability].* Zhejiang Da Xue Xue Bao Yi Xue Ban, 2012. **41**(2): p. 153-8.
48. Dev, K.K., S. Nakanishi, and J.M. Henley, *The PDZ domain of PICK1 differentially accepts protein kinase C-alpha and GluR2 as interacting ligands.* J Biol Chem, 2004. **279**(40): p. 41393-7.
49. Raveh, B., N. London, and O. Schueler-Furman, *Sub-angstrom modeling of complexes between flexible peptides and globular proteins.* Proteins, 2010. **78**(9): p. 2029-40.